Frank Zwaan (Referee)
frank.zwaan@geo.unibe.ch
In the submitted manuscript Ge et al. present a series analogue models that aim to explore different potential factors responsible for the apparent absence of the translational domain in passive margin salt tectonic systems, which contradict the current conceptual models of such systems. The model results are of high quality and would make a valuable contribution to our understanding of salt tectonics.

Please find my general comments and suggestions below. Additional comments are uploaded in the form of an annotated PDF of the manuscript.

I hope these will be helpful, please feel free to contact me for clarification.

Kind regards,

Frank Zwaan

We thank the reviewer for reading and commenting our manuscript and being so positive on it. We have prepared detailed replies to the comments as follows.

General comments
Text: The work is well written, easy to understand, concise and a pleasure to read. However, I feel it is sometimes a bit too general with opportunities to explore and explain certain topics a bit more. Therefore I would suggest to add extra description and quantification of results, background, discussion and references/comparisons with previous work at various places. These include details on sedimentation, scaling and migration of deformation. I have added specific comment below, as well as notes in the annotated manuscript.
①AUTHORS: We have addressed all aspects the reviewer commented on, including rearranging the model descriptions and improving background, discussion as well as methodology. Please find them in the revised text.

Presentation/order of model results and choice of parameters: A total of 6 “basins” (models) are presented, which are divided in three “experiments”, labeled 1a, 1b, 2aetc. I understand that the models were run in pairs, hence the labeling, but I found it rather confusing (“experiment” is singular, whereas there are 2 models, 1a, 2a, etc.looks like figure references, why not just call them models A-F or A1, A2, B1, B2, C1and C2 or so?). Also, I would suggest to consider reordering things a bit as the current organization seems a bit random; there is no obvious logical change of parameters from model to model it seems? For instance, current 2a and 2b differ in more than one factor, so presenting them together as a pair may provide a direct comparison challenging. Similarly, it may also be difficult to directly compare other models? Was this done intentionally? Are there any additional models available to bridge the gaps? (e.g. between current 2a and 3a, which have both different sedimentation patterns and different pre-kinematic layer thicknesses). Were specific models rerun to test reproducibility?
②AUTHORS: The other reviewer also raised a similar issue regarding the order of presenting the model results. So we have rearranged all the models to group them into categories of testing sedimentary cover thickness and minibasin loading to provide a more systematic comparison of different models. When designing the model, Basin 1a (or Model A in the revised text) serves as a main baseline for comparison. For example, Basin 2a (now

Model E) has same sedimentation rate as Basin 1a but with differential loading pattern. Similarly, comparing to Basin 1a (Model A), Basin 3b (Model C) has halved cover thickness at any given stage. And Basin 3a (Model F) has same cover thickness as Basin 3b but with a differential loading pattern. Moreover, we also ran other models to validate some of the thoughts presented here but with a different boundary condition, such as tilting, running time etc., therefore we only presented three experiment runs in the manuscript.

Specific comments

Scaling: could you add the equations used to obtain the scaling values in table A1, either in section 2.2 or with a bit more background in the/an Appendix? Why the distinction between subareal and submarine salt basins? These models represent submarine salt basins I assume?

③AUTHORS: We have reworked the scaling part including the addition of scaling relations and factors in the table now more rigorously. The reviewer is correct that the prototype we modelled are salt-bearing basins in a submarine setting, which is typical for most passive margin salt basins. The submarine environment has an impact on the scaling because the extra water column reduces the deformation rate. As our experiments are conducted in sub-aerial environment, this results in a modified time scaling compared to systems modelled in a sub-marine environment, which is now described more rigorously.

At some points in the methods part, the authors mention only model dimensions, where it may be helpful to add the associated natural dimensions. See also annotated PDF.

④AUTHORS: We now have reported more corresponding natural dimensions to model dimensions when describing the models.

Please add more details on the set-up (e.g. type of confinement, basal friction).

⑤AUTHORS: We have provided more details in the set-up. The silicone is confined by the sand walls and base. We have to be honest that we have no constraints on the strength of the interface between sand and silicone. The basal friction (between sand and plastic base) is not relevant here since it is high enough to prevent any slip across this interface. Please see point to point answer 11 for more details.

I suggest adding more details on how sedimentation was applied: how is the wedgescape sieved and how precise is its shape? How are the minibasin deposits applied?

⑥AUTHORS: We have added more details on sedimentation as how the pre-kinematic layer, syn-kinematic wedges and minibasins are created. The pre-kinematic layers and minibasins are relatively precise in shape. However, the sieving of wedges is loosely confined as more sediments will be put into the area with deformation and topographic low, such as extensional grabens/faults. Now we have added the relevant information in model design for clarification.

The “uniform” sedimentation in these models is characterized by aggradation rather than by progradation. I believe the latter is supposed to be more common (at least in models?). What is the reason to use an aggradational sedimentation pattern? And does it influence the results? (could you compare with previous works?)

⑦AUTHORS: We did this sedimentation pattern to exclude major influences from sediment progradation, which has been shown to have an effect on translational domain evolution previously. We point to this mechanism in the discussion (strong sediment progradation along can modify the translational domain by forward shifting of extension on previous contractional domain, McClay et al.(1998).

With the sedimentary wedge shape, we indeed put more sediments in the upslope area. However, it is worth mentioning that during actual sieving, when deformation localization occurs, such as extensional grabens, more sediments are necessary to add to those areas as they are topographic lows. Now we have added that information in the description of model design to clarify the sieving procedure. Furthermore, based on the evidences of Model D, where no differential loading was applied, the basin evolution of Model D is similar to other basins, we argue the differential sediment input has negligible impact up domain partition and kinematic evolution in our experiments (A, B etc.).

Could you add some details on minibasin formation and spacing? This is quite interesting and important I think, yet only shortly mentioned in the methods by means of a reference to other work. Is it realistic to have minibasins all over a passive margin salt basin? Widespread minibasin formation may be something more typical for e.g. the North Sea, where post-salt rifting in the Triassic caused the creation of such a setting.
⑧AUTHORS: We have added more information regarding the minibasins formation and change of sieving pattern in the relevant section. Minibasins indeed occur throughout salt basins in passive margin, but their driving mechanism can be quite different. For example, minibasins (or growth synclines) in contractional domain usually associate with contraction rather sediment loading. However, in our modelling, minibasins were created (by sediment loading) to observe minibasin influences on strain transfer between upslope extension and downslope contraction rather than to reproduce the initial development of minibasins, such as those the Central North Sea.

In the discussion, please include the work by Brun and Fort (2004) in Tectonophysics (https://doi.org/10.1016/j.tecto.2003.11.014), as well as Fort et al. (2004) in MPG (https://doi.org/10.1016/j.marpetgeo.2004.09.006), who also describe migration of deformation, even when using a thick pre-kinematic layer, which is in contrast to the results presented in this manuscript? Please make sure to cover all relevant literature ! e.g. the book chapter by Warren (2016) may prove useful (https://link.springer.com/chapter/10.1007/978-3-319-13512-0_6)
⑨AUTHORS: We have added more references in the relevant section within the discussion. Regarding the work from Brun and Fort 2004 and Fort et al., 2004, the former focuses on contractional structures and the latter discusses differential loading, therefore the two references are included in different section of discussion.

Also, please make sure to fully describe the migration of deformation in the models. It seems that only the migration of the compressional domain is addressed, whereas that of the extensional domain received little attention?
⑩AUTHORS: We have added more description on extensional domains in the result part.

I would suggest adding some more annotation to the top view figures, especially 4, 6 and 8 in order to help the reader distinguish important details. Please consider giving every sub-image its own label (a, b, c, etc.) that can be used for referencing in the text. I sometimes had some

trouble finding in the images what was described in the text. Please check further comments on Figures in the annotated PDF
⑪AUTHORS: We have revised relevant figs presenting model results as well as giving more annotations to top view maps in the text.

The link to the supplementary material does not seem to work, so I was not able to check that
⑫AUTHORS: During the review process the supplementary material is available from a temporal preview* link. The doi will be issued once the paper is accepted.
*http://pmd.gfz-potsdam.de/panmetaworks/review/36980d98249d861dabcd19b8331a044b327cf5efe25f553613dc4ef2a92756e7

The following is a point to point answer to comments on the PDF. Minor corrections in accordance with reviewer's suggestions such as choices of word are not reported unless we choose another word or phrase. Suggestions to images are all implemented and can be found in the new images. Note the page and line number (P?L?) is based on the commented (submitted) version of PDF.

1. P1L1: Although it may be correct, the title feels a bit off I think. Maybe consider: "Mechanisms of translational domain destruction in passive margin salt basins: ..."?
AUTHORS: The other reviewer also had a similar comment, we have used the word "overprinting" instead of "destructing" in the new title and other places throughout the manuscript.

2. P1L10 Maybe specify "theoretical models"? (vs. the observations from nature mentioned in the next sentence)
AUTHORS: We now have reworded it as 'conceptual models of gravitational tectonics'

3. P2L11 "supposed to be characterized"? (contrast with observations from nature)
AUTHORS: We have reworded 'characterized by' as 'typically depicted as a' (suggested by another reviewer).

4. P3L12 "originates and evolves and ascertain" rephrase.
AUTHORS: We have reworded 'originates and evolves and ascertain' as 'originates and evolves and investigate'.

5. P3L20 Please specify why such (Withjack and Callaway, 2000) materials are proper analogues for modelling salt tectonics
AUTHORS: We have added the sentence 'Quartz sand is suitable to model the supra-salt cover sediment due to its brittle nature. Similarly, silicone oil and salt both behave in a viscous manner in model and nature, respectively.'

6. P4L5 Please This however depends on the thickness of the cover (Jackson and Talbot, 1986). see Fig. 2. here:
http://cires1.colorado.edu/people/jones.craig/WUStectonics/Salt_Tectonics/index.html
AUTHORS: We agree that the density ratio between cover and salt is depth dependent. However, as demonstrated by Allen and Beaumont, 2012, the development of structures is more sensitive to overestimated buoyancy than underestimated one therefore a low density ratio is suggested. Also it is a general accepted approach to mix sand and light material to achieve light density ratio (e.g. Dooley et al., 2017).

7. P4L15 please add equations/calculations here or in appendix
AUTHORS: We have reworked the scaling section and now give the most important equations. Scaling relations and factors are now also reported more rigorously in the Table.
.

8. P4L20 This is not very clear explained. Where is the Ramberg number used?
AUTHORS: We have reworked the scaling section and make clear the role of the Ramberg number "

9. P4L23 what is "t*sm"? please specify sm

AUTHORS: Here we use ‘sm’ as short for submarine. In the revised version we use only use t* to avoid any confusion.

10. P4L30 I believe there should be more works that can be referred to (e.g. Brun and Fort 2004)
AUTHORS: We have added the suggested reference.

11. P5L1 which represents xxx km in nature? Is this relevant? It is twice the same basin? Does the sand have an effect? Is the model confined by sand on all sides? What is the friction at the base?
AUTHORS: We have completely rewritten the two sentences to make it clear.

‘Two basins of 35 cm (35 km in nature) wide and 90 cm long (90 km in nature) are built on the wedges separated by a 4 cm wide sand wall in between and bounded by two 3 cm wide sand walls on the outside boundaries (Fig. 2a). The silicone is put into the basins and confined by the sand walls (Fig. 2a).’

‘No frictional deformation occurs in the base sand wedges.’

11. P5L6 how much is this per Ma (in nature)?
AUTHORS: We have added ‘(0.17°/Ma).’ in the main text.

12. P5L10 Why 3.5˚? How much Ma does this represent? Is this static position something that we observe in nature? Is there a specific reason for the 36 hours?
AUTHORS: We have added ‘(three and half days or 21 Ma in nature).’ to make it clear. The margin tilting is generally up to a few degrees, please see Brun and Fort 2011 for more details. The static position is simply a result of ceased tilting. And the 36 hours is just a time window to observe what happen after tilting stops (e.g. the basin wide strain rate decreases). We have also added this point in the text for clarity.

13. P5L18 I would propose to call it 3 pair of models (see general comments)?
AUTHORS: We have added word the sentences as the reviewer suggested.

14. P5L23 Here and in the following it would be useful to have more specific labeling instead of generally referring to "Fig. 3"?
AUTHORS: We have added A-F in the Fig. 3 with reorganized order.

15. P5L28 How is this done? A bit more info would help the reader. Why is this? Is this transition something that is common in nature? Was sieving always done at the same location with respect to the set-up (external reference frame) or with respect to the downdip moving minibasins (sedimentation in the depocenters)
AUTHORS: Regarding to the comments above on minibasin development, we have rewritten the part of model setup to give more details on why and how we built the minibasins. Essentially, we created the minibasins by sieving an extra layer of cover material along strike, on a string in the silicon basin to create minibasin downbuilding. We did such differential sieving in first three rounds during which the extra sediments were put on the exact location of the minibasin. However, afterwards, we shifted to more regular sieving of wedge shape sedimentation as the differential loading pattern had been established.

16. P6L5 Two parameters that differ with respect to previous models, difficult to compare with previous models...!
AUTHORS: We have reorganized the order of the models as mentioned above.

17. P6L20 Is it possible to be more accurate than the pixel size?
AUTHORS: We have used 0.1 mm instead of 0.1 px to give a more straightforward evaluation of the resolution.

18. P6L23 Can Vx and Vz be used to quantify and discuss deformation in the models? I believe for now it is only used for map view pictures? Why not use it?
AUTHORS: We agree it is an important question as different dataset highlight different characteristics of the model. In general, Vx is useful to highlight the translational domain and Vz is good at showing the salt outflow and inflow. However, they are not as good as strain in showing the structural and kinematic evolution of the silicon basin. Therefore, we only show Vx and Vz as map view in the results. Now we have added some of the information mentioned above into the main text.

17. P7L6 Ma in nature?
AUTHORS: We have revised the text as '25–36 hours (7–9 Ma in nature), 61–72 hours (16–18 Ma in nature) and 109–120 hours (28–30 Ma in nature)' to show the corresponding time in nature.

18. P7L26 Please add more details on the extensional domain and its evolution.
AUTHORS: We have added 'Afterwards, the extensional domain continues to expand to the end of the experiment, reaching to over 20 cm wide (Figs 4b, c and 5a).' in the revised text to describe the extension evolution of Model A (previous Basin 1a). We also added more details of extension of Model B, C and F (previous Basin 1b, 3b and 3a) in the text as well.

19. P8L6 and P8L10 Can you indicate this on the image? Please specify. I assume the diapirism causes the extension seen between the passive minibasins? Please annotate in the Figure
AUTHORS: We have indicated the diapirs in Fig. 9a and b.

20. P8L21 quantify??
AUTHORS: We have replaced the phrase ' late stage' with more precise time 'after 72 hours'.

21. P8L33 Where can we see this??
AUTHORS: We have added annotation on Fig. 9b to highlight the impact of differential loading.

22. P9L25 Please add references here
AUTHORS: We have added relevant references in the sentence.

23. P10L7 Yet Brun and Fort have very different results!?
AUTHORS: In Brun and Fort 2011, in their dominant gliding model (Fig. 15), there is a clear translational domain between upslope extension and downslope contraction. Although it is less obvious in the model of Fig. 10.

24. P10L15 Please compare with Brun and Fort 2004 and potential other works?

AUTHORS: We have compared the characters of thick cover strata to other experiments, such as Brun and Fort 2004, where the translational domain gets preserved.

25. P10L20 So that we should expect prograding systems? How well does this fit with the sedimentation applied in this work?
AUTHORS: As we have mentioned above, our sedimentation pattern is not entirely aggradation. Structures with topographic lows receive more sediments during sieving. Moreover, Model D has negligible sedimentation shows the basin evolution is similar to those with wedge shaped syn-kinematic sedimentation.

26. P10L23 Please check Brun and Fort 2004?
AUTHORS: We have commented the reference in point 24, indicating that upslope migration with thick cover can preserve the translational domain instead of overprinting it completely (with thin cover layer).

27. P11L1 This would be information on minibasin formation and shape that should be mentioned before as well?
AUTHORS: We have used the variation of sedimentary systems to justify the creation of minibasins in the model. However, we did not model the minibasins specifically tied to any sedimentary systems or their geometries, such as models showed by Banham and Mountney 2013 on Sedimentary Research where fluvial distributary system dominates minibasin formation. In other words, differential loading in nature may be more irregular in shape than the generic geometry we used in the model. Therefore, we feel it is more reasonable to put the information in discussion rather than in the model design of minibasin creation.

28. P11L7 This may be, but is it realistic to have such large minibasin deposits over hundreds of km (the typical width of a passive margin salt basin). Minibasins may be more dominant in for instance the North Sea, which is not a typical passive margin setting. Here minibasins are formed during post-salt rifting in the Triassic. Maybe differential loading is more likely in the case of a prograding sediment wedge (e.g. Gulf of Mexico?) This should be discussed?
AUTHORS: As we mentioned before point to point answer session, the minibasins are created as differential loading to observe their behaviour during the experiments, we did not try to model a specific case as North Sea. And even in North Sea, there are also some evidences within the minibasins suggesting gravity gliding (see Karol et al, 2014 in Interpretation).

29. P11L24 I believe also Oriol Ferrer in Barcelona has done similar work that could be referred to?
AUTHORS: Thanks. We have added Oriol's Interpretation paper into the references.

30. P12L14 please specify in which part of the system where the loading is most significant
AUTHORS: We have now pointed out that early loading in the mid-slope is important to deform the translational domain.

Tim Dooley (Referee)
tim.dooley@beg.utexas.edu
Received and published: 2 April 2019
This manuscript uses physical models to assess the formation, deformation and overprinting of translational domains on gravity-driven salt-cored passive margins. I like the models in general and they should be useful to people interested in salt tectonics.

Tim Dooley

We thank the reviewer for reading our manuscript and for the constructive comments. We have addressed all the issues in this file and file attached.

General comments:
These experiments follow on from several papers published since 2017 on the impact of base-salt relief on deformation on these types of margins and are thus quiet timely. These other studies used physical models, numerical models and seismic-based studies. I think the authors should refer to these in the introduction and state the differences, and similarities, between those studies and their own, rather than just adding this in as a footnote at the end of the manuscript.
AUTHORS: We have expanded the introduction of previous work on how base-salt relief influences translational domain deformation and compare the similarities and differences.

My main problem with the manuscript is the presentation of results. There are 3 experiments with essentially 2 basins in each experiment, and the authors present them in pairs. There is no need to do this. There are 6 distinct experiments as there was no connectivity between the "basins". Split these up so that you can present the parameters you tested in a logical fashion. See the comments on the manuscript for more details but you can work it like so:
1. Evaluating sediment thickness controls on size of translation zone
2. Evaluating sediment depositon rates on translation zones – but use strength
3. Evaluating discontinuous loads on translation zones
AUTHORS: The other reviewer also mentioned this problem. We have rearranged the models to group them as the reviewer suggested: one is on sediment thickness and deposition rate and the other is on sediment loading. Please find the detailed changes in the attached file.

I also feel that some areas of the text need expanding on, and others are perhaps too wordy. See the comments on the PDFs.
AUTHORS: We have addressed all the points the reviewer has raised in the PDF.

The following is a point to point reply to the comments in the PDF. Minor corrections in accordance with reviewer's such as choices of words or phrases are not reported unless we choose another word or phrase. Suggestions to images are all implemented and can be found in the new images. Note the page and line number (P?L?) is based on the commented (submitted) version of PDF rather than revised one.

1. P2L8: Well the whole point of Dooley et al. (2017) was to point out that base-salt rugosity impacts the extension-translation-contraction model. But in broader terms that still generally defines these salt-cored margins.
AUTHORS: Exactly, that is why we referenced it here. Also, the model of fig.1 in of Dooley et al 2017 is exactly showing the conceptual model with kinematic partition of extension, translation and contraction.

2. P2L10: Well yes but 3 papers by myself and coworkers focused on modified strain histories in translational domains due to the effects of base-salt relief. Also new studies by Pichel et al. using numerical models and seismic-based studies in the Santos Basin.
AUTHORS: We have discussed the influence of base-salt relief on modifying translational domain with related references as follows:

'Recent studies have shown that base-salt relief can initiate extensional and contractional structures as well as ramp syncline basins therefore modify the translational domain (e.g. Dooley et al., 2017; Dooley et al., 2018; Ferrer et al., 2017; Pichel et al., 2018). However, in basins where pre-salt relief is limited or very gentle (e.g. Fig. 1b and c), such as the Lower Congo Basin, other mechanism may be responsible for modifying the translational domain.'

3. P2L28: *'When used as a term describing the basin-wide structural partitioning, the translational domain usually indicates an area located between the upslope extensional and downslope contractional structures (e.g. Fig. 1a).'* Yes, that's what people mean.
AUTHORS: According to this definition, translational domain indicates an area between extension and contraction. As we mentioned in the text, extension and contraction can intervene due to upslope migration of contraction, and thus the translational domain may disappear during the basin evolution, even with a large undeformed block in the mid-slope (e.g. Fig. 7a in the revised text). Therefore, we feel this definition alone is too vague and does not really depict the conceptual model well.

4. P3L26: There are other studies using DIC...
AUTHORS: We have added more recent references as well as put 'e.g.' to indicate there are more similar work with DIC method.

5. P3L29: Need some references here – main work by Ruud Weijermars on scaling properties of PDMS for rock salt in experiments.
AUTHORS: We have added relevant references in the text.

6. P5L8: *'Each of the experiments takes about ten days from preparation to slicing. The silicone is filled in the silicone basin at least 3 days to settle'* Not really required.
AUTHORS: We have shorten the sentence to 'The silicone is filled in the silicone basin.'

7. P5L14: *'During the experiment, the granular material is added by sieving within about twenty minutes onto the model surface every 12 hours to simulate syn-kinematic*

sedimentation (Appendix Table A2). After the experiment, the model surface is covered with sand before being gelled, sliced and photographed.' Rewrite this. Take out unnecessary stuff. Use appendix for some of these details.
AUTHORS: We have revised the sentences to 'During the experiment, the granular material is added by sieving every 12 hours to simulate syn-kinematic sedimentation (Appendix Table A2). After the experiment, the model is sliced and photographed for cross section view.'

8. P5L20: So it's a mixture of gliding and spreading with wedges. Needs some discussion.
AUTHORS: The other reviewer also raised a similar point. In our experiments. The pre-kinematic layer is sieved evenly, so only the syn-kinematic wedge is sieved with thickness variation. However, the wedge shape of sedimentation in Fig. 3 is just a guideline. During the experiments, areas with deformation, such as extensional structures, receive more sedimentation due to their topographic reliefs. Therefore the differential sieving is not only a driven force but also a sedimentation response to gravity gliding. Moreover, it is also evident from Model D (no differential loading) that the basin has kinematic partitions and structural evolution as the ones with wedge shape syn-kinematic sedimentation. We have also added relevant details into text to clarify the issue. Please also refer to answer ⑦ in review 1's reply.

9. P5L24: Rewrite this for clarity and use figures.
AUTHORS: We have reorganized the description of model designs.

10. P5L28: *'Minibasin spacing and dimensions are constrained by generalization of natural observations (Cramez and Jackson,2000; Hudec and Jackson, 2004; Marton et al., 2000).'* Expand on this..
AUTHORS: We have given more details of rational of minibasin creation as well as technical details of creating them in the main text. Please also refer to answer ⑧ in reply to review 1.

11. P6L13: *first paragraph of Experimental monitoring*. Can be shortened
AUTHORS: We have shorten the paragraph a bit.

12. P6L23: This makes it sound like Vx is subsidence and Vz is uplift. Rephrase.
AUTHORS: We have revised the text as 'horizontal displacement (Vx) showing downslope movement and vertical displacements (Vz) reflecting salt outflow and inflow.'.

13. P7L1: *first paragraph of Experimental results* Is all this necessary?
AUTHORS: We feel such paragraph may help reader who are not familiar with modelling get an idea of the presentation of results.

14. P7L11: The use of "Experiment 1" is awkward as there are 2 experiments in here.
AUTHORS: We now have reorganized the order of models in order to avoid such situations.

15. P7L17: Thicker/stronger roof favors flow within the salt layer – Poiseuille flow. Salt-flow-driven uplift is seen at the downdip edge of the basin which you don't even mention.
AUTHORS: We now have briefly mentioned the uplift due to silicon flow in Model B. However, as the manuscript focuses on the translational domain evolution and the subsidence and uplift displacement have similar patterns across different models, we feel a very detailed description of subsidence and uplift is beyond the scope of this study. Moreover, we feel we are not in a position to comment on the silicone flow type, either Poiseuille or Couette flow, as we did not monitored the silicone flow directly.

16. P7L20: *'In Basin 1b, major deformation starts in the mid stage when a thrust belt Tb1 occurs c. 10 cm away from the silicone basin tip in the downslope'* Rephrase.

P7L25: *'At the same time in Basin 1a, the thrust belt shifts towards the basin tip of the downslope as well as the upslope and both thrust belts keep active into the late stage (εxx in Fig. 5a).'* Rewrite this

P8L1 *'In Basin 2a, differential loading of the prekinematic layer and early syn-kinematic sieving results in a basin-wide imprint of minibasins downbuilding, as shown by the subsidence pattern during the early stage where strings of thicker pre-kinematic layer subside stronger than intervened regions forming minibasins'* Rewrite for clarity

P8L8 *'During the transition, the minibasin area (apart from Minibasin 1) becomes a shadow zone of deformation and transfer strain passively while the diapirs start to accommodate deformation (Fig. 7c).'* Not clear
AUTHORS: We have reworded the relevant text

'Major deformation starts in the mid stage when extensional domain occurs in the upslope with c. 10 cm width (Fig. 4e). In the meantime, a thrust belt T_{b1} occurs c. 10 cm away from the basin edge in the downslope (Fig. 5b).'

'In the mid stage (after 48 hours), the thrust belt shifts towards both upslope and downslope with all thrust belts being active in the late stage (ε_{xx} in Fig. 5a)'

'In Model E, differential loading of the pre-kinematic layer and early syn-kinematic sieving (with 8 minibains) results in a basin-wide imprint of minibasins downbuilding. The differential loading process is most prominent on the subsidence pattern during the early stage where thicker minibasin areas subside stronger than intervened regions forming minibasins (Vz in Fig. 8a)'

'During the transition, the minibasin area (apart from Minibasin 1) are lack of internal deformation while the diapirs in between start to accommodate deformation (Fig. 9c).'

17. P8L5: Annotate this on the figure. It's not clear to people unfamiliar with this type of data.
AUTHORS: We have annotated early stage minibasin development on Fig. 9c.

18. P9L20: *'i) migration of extensional and contractional domains into a previous undeformed translational domain; ii) differential loading by sedimentation into minibasins that triggers salt-related structures, such as diapirs, from the beginning of basin evolution therefore prevents the formation of a tectonically stable translational domain.'*
But it does form. Local weaknesses can allow jostling and squeezing etc. but the translational domain exists. It's just not a nondeformed zone. And extension can propagate into it as well.
AUTHORS: As we mentioned in point 3, if the translational domain, whether it is deformed or not, only indicates an area between the extension and contraction, then translation is a time-dependent concept. As shown in Model A and C (Figs 5a and 7a), the contraction can migrate to the location that just next to the extension. As defined above, the translational domain does not exist anymore. Moreover, such definition provides no diagnostic structural evidence that can help us recognize translational domain in nature. Therefore, we had defined

the translational domain with character as undeformed to make it practical to discuss why such undeformed domain does not occur in nature.

19. P9L25: *'sedimentation rate'* In reality you're are not scaling a sedimentation rate as the layers are basically added instantaneously. Use roof strength as a proxy for that.
AUTHORS: We agree that syn-kinematic layers are added instantaneously so they are not exactly sedimentation rate. However they are not only cover strength as well. We have use the phrase 'sedimentation pattern' instead.

20. P10L5: *'According to our study, a 1 mm 5 thick pre-kinematic layer and 2-3 mm sediment from syn-kinematic sedimentation (few hundreds of meters if scaled to nature) seems strong enough to form a stable translational domain from beginning to end, such as in Basin 1a (Fig. 5a).'*
So does 1B - very large unstrained domain in Figure 5.
AUTHORS: We have added a short discussion on Model B (Basin 1B) on its thicker cover.

'With a thicker cover, such as Model B (5 mm pre-kinematic layer), the translational domain gets even larger (c. 55 cm wide) due to stronger cover (Fig. 5b).'

21. P10L22: Well it could occur if margin tilt is modified during late-stage evolution of the margin – like in Kwanza basin.
AUTHORS: We have added the relevant discussion of Kwanza Basin on its sub-salt uplift of upslope area and downslope migration of extension.

22. P10L33: You're adding load in a linear fashion, perpendicular to the slope so that has an impact.
AUTHORS: We have indicated that the minibasins are idealized as strings in shape.

23. P11L15: *'A translational domain therefore is not necessary to be present during the whole evolution of the passive margin salt basins.'*
Yes, perhaps, but it still forms the translational domain, i.e. not in a zone of continuous shortening nor in a region of regional extension. This would also depend on teh orientation of diapirs in how they take up strain.
AUTHORS: We explained the reason in points 3 and 18 that the definition of translational domain between extension and contraction is not very practical. We agree that the orientation of diapirs influence the strain distribution. We have added the importance of diapir orientation into the text.

24. P11L25: *'Moreover, progradational sedimentary wedges can also prevent the translational domain from forming. As the sedimentary wedges progressively move basinwards, early formed contractional structures are superimposed by late extensional structures, completely destroying the translational domain (Brun and Fort, 2011; McClay et al., 1998; Vendeville, 2005). Although the sedimentary wedge is also one type of differential loading, the absence of tilting makes the system very different 30 from the ones presented in this study. Future research therefore is needed to fully understand the influences of sub-salt structures and progradational wedges on the development and destruction of translational domains.'*
Not very clear here.
AUTHORS: We have revised the paragraph to make it clear.

25. P12L1: on Conclusions
Models should be described discussed as:
1. Evaluating sediment thickness controls on size of translation zone
2. Evaluating sediment depositon rates on translation zones
3. Evaluating discontinuous loads on translation zones
AUTHORS: We have clarified the influences of cover thickness on translational domain evolution. However, we think it is difficult, if not impossible, to evaluate the sediment thickness and deposition rate completely separately because high sedimentation rate leads to thick cover layer.

26. P12L16: Refer to other reasons for deformation within this domain. Published work.
AUTHORS: We have indicated other reasons for translational domain deformation in the discussion.

~~Mechanisms of destructing~~Overprinting translational domains in passive margin salt basins: Insights from analogue modelling

Zhiyuan Ge[1]*, Matthias Rosenau[2], Michael Warsitzka[3,2] and Rob L. Gawthorpe[1]

[1] Department of Earth Science, University of Bergen, Allégaten 41, 5007 Bergen, Norway
[2] Helmholtz Center Potsdam, German Research Center for Geosciences - GFZ Potsdam, Germany
[3] Institute of Geophysics of the Czech Academy of Sciences, Boční II/1401, 141 31 Prague 4, Czech Republic

Correspondence to: Zhiyuan Ge (Zhiyuan.Ge@uib.no)

Abstract. Current models of gravitational tectonics ~~models illustrating~~on the structural styles of salt-influenced passive ~~margin salt basins~~margins typically ~~have~~depict domains of upslope extension and corresponding downslope contraction~~,~~ separated by a mid-slope domain of translation that is rather undeformed~~ mid-slope translation.~~. However, ~~such a~~an undeformed translational domain is rarely observed in natural systems ~~where~~as extensional and contractional structures ~~may~~tend to interfere in the mid-slope area. In this study, we use sandbox analogue modelling analy~~z~~sed by~~ 4D~~ digital image correlation (DIC) to investigate ~~how~~some of the ~~pre-kinematic layer thickness, differential sediment loading and sedimentation rate~~factors that control the structural evolution of translational domains. As in nature, experimental deformation is driven by slowly increasing gravitational forces associated with continuous basal tilting. The results show that a translational domain persists throughout the basin evolution when the pre-kinematic layer is evenly distributed~~,~~. Although a thin (1 mm in the experiment, 100 m in nature) pre-kinematic layer can render the translational domain relatively narrow when comparing to settings with a thicker (5 mm) pre-kinematic layer. In contrast, early differential sedimentary loading in the mid-slope area creates minibasins ~~intervened~~separated by salt diapirs overprinting the translational domain. Similarly, very low sedimentation rate (1 mm per day in the experiment, ~~equates to~~ < 17 m/Ma in nature) in the early stage of the experiment results in ~~an immature~~a translational domain quickly overprinted by downslope migration of the extensional domain and upslope migration of the contractional domain. Our study suggests that the architecture of passive margin salt basins is closely linked to the ~~sedimentary~~pre- and syn-kinematic cover thickness~~ and sedimentation pattern and rate.~~. The translational domain, as an undeformed region in the supra-salt cover, is ~~likely~~ a transient feature ~~in nature~~ and ~~destructed~~overprinted in passive margins with either low sedimentation rate or a heterogeneous sedimentation pattern.

Keywords translational domain, thin-skinned, salt tectonics, passive margin, analogue modelling,

digital image correlation (DIC)

1. Introduction

In passive margin basins containing syn- and post-rift salt deposits, salt tectonics generally have significant influences on structural style and stratigraphic architecture (e.g. Jackson and Vendeville, 1994; Rowan, 2014; Tari et al., 2003). ~~As the margin tilts~~ Tilting due to thermal subsidence or seaward progradation of sedimentary wedges causes passive margin salt basins to experience deformations related to gravitational failure, typically forming a linked system of upslope extension and downslope contraction separated by a more or less undeformed, translational domain in the mid-slope (e.g. Brun and Fort, 2011; Cramez and Jackson, 2000; Dooley et al., 2017; Fort et al., 2004a; Rowan et al., 2004) (Fig. 1a).

The translational domain has received relatively limited attention whereas the extensional and contractional domains have been studied extensively. The translation domain is generally considered to be a rather passive region of the cover strata, which remains largely undeformed during basin-wide gravitational gliding and spreading (Fig. 1a) (e.g. Adam et al., 2012a; Dooley et al., 2017; Fort et al., 2004a). However, sub-surface data generally show evidence of deformation within the mid-slope areas of translational domains in most passive margin salt basins, such as those in the West Africa and Brazilian margins (e.g. Marton et al., 2000; Modica and Brush, 2004) (Fig. 1b and c). To our best knowledge, only one subsurface study so far has interpreted an overall undeformed translational domain based on 2D regional seismic analysis (Gradmann et al., 2005). However, this interpretation has been challenged more recently based on high-quality 2D and 3D seismic analysis, which suggests widespread faulting in the translational domain (Gvirtzman et al., 2015). Most passive margin salt basins have typical structures of minibasins and salt diapirs in the mid-slope, translational domain area (Fig. 1b and c).

~~While the translational domain has received little attention so far, the extensional and contractional domains have been studied extensively. For example, numerous studies have focused on structural style and kinematic evolution of rotated fault blocks (Mauduit et al., 1997), rollovers (Krézsek et al., 2007; Mauduit and Brun, 1998) and extensional diapirs (Koyi, 1998; Vendeville and Jackson, 1992a, b) in the extensional domain, and folds and thrusts~~ Recent studies have shown that base-salt relief can initiate extensional and contractional structures as well as ramp syncline basins in the mid-slope therefore modify the translational domain (e.g. Dooley et al., 2017; Dooley et al., 2018; Ferrer et al., 2017; Pichel et al., 2018). However, in basins where pre-salt relief is limited or very gentle (e.g. Fig. ~~, salt nappes and canopies~~ (Hudec and Jackson, 2009, 2004; Masrouhi et al., 2013; Rowan et al., 2004)~~ in the contractional domain. Conceptual models of salt-bearing passive margins commonly reduce the translation domain to a rather passive region of the cover strata, which widely remains undeformed during basin wide gravitational gliding and spreading (Fig. 1a)~~ (e.g. Adam et al., 2012a; Fort et al., 2004a)~~. However, sub-surface data lacks evidence of such a clear undeformed translational domain in most passive margin salt basins, such as those in the West Africa and Brazilian margins (Fig. ~~1b and c), other mechanisms may be responsible for overprinting the translational domain.

The concept of a translational domain is rather loosely defined because it has both ~~structural~~spatial and kinematic meanings. When used as a term describing the basin-wide structural partitioning, the term translational domain is usually ~~indicates~~ used to indicate an area located between the upslope extensional and downslope contractional structures (e.g. Fig. 1a). For example, when describing the structural characteristics of the Lower Congo Basin, ~~Rowan (2014)~~ used the term of translational domain to indicate the mid-slope area of salt minibasins and diapirs. Yet many diapirs and minibasins in the mid-slope have an extensional or contractional origin, due to the down- and up-slope migration of extensional and contractional domains~~, respectively~~ (Brun and Fort, 2011; Fort et al., 2004a)~~.~~ (Brun and Fort, 2011; Fort et al., 2004a). When ~~one refers~~referring to the kinematic behaviour of the salt basin, ~~the~~ translational domain ~~means~~is used to define a zone within the salt basin that is transferring the deformation without ~~internal deformation~~being internally deformed ~~(e.g. Adam et al., 2012a)~~. In this sense, the translational domain may not be part of the final basin architecture, but ~~only present during~~ is a transient feature of the basin evolution. ~~To avoid any confusion, we refer the~~ In this paper, a translational domain ~~here satisfying~~satisfys two criteria, i.e. being a largely undeform~~ing~~ed (at least transiently) area and connects upslope extension and downslope contraction.

In this ~~study~~paper, we ~~aim to~~ investigate the structural evolution of ~~the~~a salt-bearing passive margin's mid-slope area and the origin of a translation domain~~ in a salt basin setting.~~. Using ~~analogue~~ sandbox modelling combined with quantitative surface deformation monitoring by means of 4D (3D plus time) DIC (digital image correlation), we demonstrate how the translation domain originates and evolves, and ~~ascertain~~investigate possible mechanisms ~~on how~~that may overprint it ~~can be destroyed~~ during ongoing ~~gravity gliding.~~gravitational defromation. Specifically, we focus on the influences of pre- and syn-kinematic layer thickness~~,~~ and differential sedimentary loading~~ and sedimentation rate~~ on the structural evolution of the translation domain. Furthermore, we investigated the overall evolution of different kinematic domains (extensional, translational and contractional) to understand the~~ir~~ir complexity ~~of kinematic domains~~ and how they develop ~~through time and~~in space and time.

2. Analogue modelling methods

Analogue experiments ~~of gravitationally driven salt tectonic processes~~ using ~~granular rock~~ analogue materials, such as quartz sand ~~to model the supra-salt cover sediment~~ and silicone oil ~~to model salt layers~~, have been traditionally e~~x~~mplo~~r~~yed to ~~get~~gain insight into gravity-driven, thin-skinned salt tectonics (e.g. Ge et al., 1997; Mauduit and Brun, 1998; Mauduit et al., 1997; Rowan and Vendeville, 2006; Vendeville and Jackson, 1992b)~~, as well as basin-scale geometry and evolution~~ (Adam and Krezsek, 2012; Fort et al., 2004a)~~. In the last decade, the advent of quantitative and high resolution 4D DIC (digital image correlation) techniques, which records time series of incremental experimental surface deformation in 2D and 3D, allows the analysis and reconstruction of the kinematic evolution of basin-wide structures in high detail and accuracy (Adam et al., 2012a; Adam and Krezsek, 2012).~~

. Quartz sand is suitable to model the supra-salt cover sediment due to its brittle behaviour. Similarly, silicone oil and salt both behave in a viscous manner in model and nature, respectively. In the last decade, the advences of quantitative and high resolution “4D” (three spatial dimensions plus time) DIC (digital image correlation) based deformation monitoring techniques, which record time series of incremental experimental surface deformation, allow the analysis and reconstruction of the kinematic evolution of arrays of structures in great detail and accuracy (e.g. Adam et al., 2012a; Adam and Krezsek, 2012; Dooley et al., 2018; Warsitzka et al., 2015).

2.1 Rock analogue materials

In this study, we use a mix of granular materials to simulate the brittle sediment layer cover and PDMS (polydimethylsiloxane) silicone oil to represent the ~~viscous salt underneath. The density contrast between commonly used pure quartz sand and silicone~~underlying viscous salt (e.g. Weijermars et al., 1993; Withjack and Callaway, 2000). The density contrast between commonly used pure quartz sand and silicone oil in analogue modelling is generally too high when comparing to natural prototypes ~~(Allen and Beaumont, 2012)~~. In unison with other studies (Adam et al., 2012a; Dooley et al., 2007), we hereby use a mixture of quartz sand (G12, grain size: <400 µm, Rosenau et al., 2018) and foam glass spheres (company: LIAVER, grain size: 250~~-~~–500 µm, Warsitzka et al., 2019) to adjust the density ratio between the cover layer and silicone. The weight ratio for a mixture of sand and foam glass sphere is 3:1 and the resulted mixture density is 1.13 g/cm^3 after sieving~~.~~ (Table 1). The resulting density ratio between the granular mixture and silicone is 1.16, which is representative for a density ratio between cover sediments and underlying salt (e.g. Adam et al., 2012a; Allen and Beaumont, 2012; Warsitzka et al., 2015).

The frictional properties of the granular mix are similar to pure quartz sands used in analogue modelling (e.g. Klinkmüller et al., 2016). Static and sliding friction coefficients of the granular mixture are about 0.7 and 0.55, respectively, and the cohesion is in the order of few tens of Pa as determined by using a ring shear tester ~~(Schulze RST-01.pc, Schulze reference, for more details see~~ Warsitzka et al. (2019)~~).~~(Warsitzka et al. (2019) (Table 1). The silicone oil used in the experiments (Bayer Korasilon G30M) has a density of 0.97 g/cm^3 at room temperature of ~~25~~23°C with a Newtonian viscosity of about 2×10^4 Pa s at shear rates below 10^{-1}s^{-1} ~~(Rudolf et al., 2016) as realized in the experiments reported here.~~ (Table 1).

2.2 Model scaling

Adequate scaling of the analogue model from ~~the natural prototype~~nature allows a direct comparison between the model and ~~the natural prototype~~nature in terms of geometry, kinematic evolution as well as the deformation driving and resisting forces (e.g. Costa and Vendeville, 2002; Hubbert, 1937; Ramberg, 1981). Based on dimensionless numbers representing ratios of forces, scaling factors for the basic dimensions of length, mass and time are derived. Here we use the ratio ~~of lithostatic pressure vs. cohesion and the Ramberg number relating gravitation and viscous strength to derive scaling factors (e.g. Adam and Krezsek, 2012; Gemmer et al., 2005). Among all the scaling factors, the geometric (l*) and time (t*sm) scaling factors are particularly important to understand the model design and interpretation. In this study, the geometric scaling, as constrained by cohesion and densities of the rock analogue versus rocks is l* = 10-5 (1 cm in model is 1 km in nature). The time scaling, dictated by the viscosity of salt versus PDMS, is then t*sm = 4.255 × 10-10 (4 hours in the model is approximately 1 Ma in nature). See Appendix Table A1 for scaling relations.~~Γ of lithostatic pressure vs. cohesion (C)

$$\Gamma = \rho g l / C \qquad (1)$$

where ρ, g and l are density, gravitatinal acceleration and length, respectively, to scale the brittle regime and the ratio between lithostatic pressure and viscous strength (the so-called Ramberg Number Ra)

$$Ra = \rho g l^2 / \eta v \qquad (2)$$

where η and v are dynamic viscosity and velocity, respectively, to scale the viscous regime (e.g. Adam and Krezsek, 2012; Gemmer et al., 2005). Achieving the same Γ and Ra in the model as in nature ensures geometric, kinematic and dynamic similarity between the analogue model and nature (e.g. Costa and Vendeville, 2002; Hubbert, 1937; Ramberg, 1981) and allows the derivation of scaling factors for all relevant dimensions and parameters. Among the scaling factors, the geometric (l^*) and time (t^*) scaling factors, where * marks the ratios of model vs. natural values, are particularly important to design the model and interpret modelling results. From equations (1) and (2), it follows that for brittle-viscous models, the time scale depends directly on the initial choice of length scale, density and viscosity:

$$t^* = \rho^* g^* l^* / \eta^* \qquad (3)$$

In this study, the geometric scaling bounded by the cohesion and densities of the rock analogue versus rocks, is chosen as $l^* = 10^{-5}$ (1 cm in model is 1 km in nature) (Table 1). The time scaling, dictated by the density of sediments and the viscosity of natural salt versus silicone oil and strain rate, is consequently $t^* = 4.255 \times 10^{-10}$ after adjustment for submarine systems (4 hours in the model is approximately 1 Ma in nature) (Table 1).

2.3 Experimental setup and model design

~~As this study aims to~~ The overall model setup shares the characteristics of earlier studies aiming to understand kinematic domain partition and evolution in passive margin salt ~~basin, the overall setup of the apparatus shares the characteristics of earlier studies~~ basins (Fig. 2) (e.g. Adam et al., 2012a; Brun and Fort, 2004; Fort et al., 2004a). A flat rigid base of 1 m wide and 1.8 m long is covered by a ~~basal sand layer with a~~ double-wedge shape basal sand layer that serves as a mould for the basin fill akin to passive margin basins ~~(Brun and Fort, 2011, 2012).~~(Brun and Fort, 2011, 2012). The two wedges are 65 cm in the upslope and 25 cm in ~~length and 90 cm wide~~the downslope respectively (Fig. 2a). ~~The asymmetric basin formed by the~~ In each experiment, we simulate two basins, each 35 cm wide (35 km in nature) and 90 cm long (90 km in nature), built on the basal wedges ~~is subdivided~~separated by a 4 cm wide sand ~~ridge along its symmetry axis separating two 35 cm wide and 90 cm long asymmetric basins filled with silicone (Basin a~~wall and ~~Basin b)~~bounded by two 3 cm wide sand walls on the outside boundaries (Fig. 2a). The ~~silicone thickness~~basin depth is 2 cm at the basin's deepest location and pinches out upslope and downslope towards the ~~basins margins~~basin edges (Fig. 2a). The tilting of the entire base and model towards the ~~steeper basin~~ side ~~as downslope~~ of the short wedge is driven by a computer-controlled stepper motor at a continuous rate of 1° ~~per day~~/day (0.17°/Ma) (Fig. 2b). Importantly, no deformation occurs within or at the base of the basal sand wedges during the experiment.

~~Each of the experiments takes about ten days from preparation to slicing. The silicone is filled in the silicone basin at least 3 days to settle.~~The basin is filled with silicone and once the silicone is free from air bubbles and has a flat upper surface, a pre-kinematic layer of the quartz sand – foam glass beads mixture is sieved onto the ~~silicone~~basin surface. Then, tilting is started at the rate of 1 ° per day until reaching a final tilting ~~position~~ of 3.5~~°~~° after 84 hours~~.~~ (three and half days; 21 Ma in nature). Subsequently, the experiment continues for another 36 hours to observe basin evolution under static, tilted conditions. The total running time is ~~consequently~~ 5 days or 120 hours, which equals to approximate 30 Ma in ~~the natural prototype~~nature (Appendix Table ~~A2~~A1). During the experiment, the granular, cover material is added by sieving ~~within about twenty minutes onto the model surface~~ every 12 hours to simulate syn-kinematic sedimentation (Appendix Table ~~A2~~A1). After the experiment, the model ~~surface is covered with sand before being gelled,~~ is sliced and photographed for cross sectional analysis.

~~Overall~~ Three experiments, each with two basins, were ~~carried out~~performed for ~~the purpose of~~ this study ~~and~~(Fig. 2a). Sedimentation patterns were ~~varied~~different for the ~~two sub-~~modelled silicone basins ~~throughout~~(Fig. 3). We group the modelling results into two categories with Model A–D focusing on the ~~three experiments:~~

~~Experiment 1 (basins 1a~~influences of cover thickness and sedimentation rate and~~1b)~~, Model E and F emphasizing the role of minibasin loading on translational domain evolution:

1. Model A aims to ~~investigate~~establish a baseline for investing the impact of sedimentation pattern and rate on the evolution of the translational domain. In Model A, the pre-kinematic layer ~~thickness on the development of the translational domain. In Basin 1a, the pre-kinematic layer was~~is 1 mm thick and further sedimentation ~~was~~is added every 12 hours with an overall wedge shape and 1 mm average thickness (Fig. ~~3). Basin 1b had~~3a). The wedge-shape sedimentation, which thins downslope, mimics proximal sediment source areas and overall reduction in downslope sedimentation. Moreover, when deformation occurs creating extensional grabens or contractional folds, more materials are added over structures with topographic lows to mimic natural sedimentation. Such sieving method is also applied for other models.

~~1.~~2.Model B has the same syn-kinematic sedimentation rate as the ~~Basin 1a~~Model A, but with a pre-kinematic layer of 5 mm~~(~~, in order to study the influences of pre-kinematic layer thickness on the translational domain evolution (Fig. 3b~~Fig. 3~~).

3. ~~Experiment 2 (basins 2a and 2b) tests how differential loading and minimum sedimentation influence the translational domain. The~~ Model C investigates the translational domain development under reduced pre-kinematic layer thickness (0.5 mm) and sedimentation rate (0.5 mm per 12 hours) (Fig. 3c) comparing to Model A.

4. Model D has an even thickness of 1 mm for the pre-kinematic layer (Fig. 3d). Further sedimentation is only added when necessary to cover the newly exposed silicone. Therefore, Model D has negligible syn-kinematic sedimentation ~~was~~and provides an extreme example of translational domain evolution under sediment-starved condition with no significant influence from sedimentary differential loading.

~~2.~~5. Model E studies how differential loading influences the ~~same as in experiment 1~~translational domain (Fig. ~~3). However~~3e). Specifically, the pre-kinematic layer in ~~Basin 2a was 1 mm thick in~~Model E has an average thickness of 1 mm, but with a differential sedimentation pattern of 8 minibasins created by sieving. We sieve an layer of sand, up to 1 mm thicker than the surrounding areas to create the minibasins. The minibasins ~~we~~are 3–4 cm wide with 6–7 cm gaps in between. The differential sieving continues for another three rounds before sieving shift to sedimentary wedges shape (Fig. 3e), because previous studies have suggested that differential loading is more likely to dominate the thin-skinned deformation system during the early stages of basin evolution (e.g. Adam et al., 2012a). Minibasin spacing and dimensions are constrained by generalization of natural observations where they can be a few kilometres to tens of kilometres in diameter and intervened by salt diapirs of similar size (e.g. Cramez and Jackson, 2000; Hudec and Jackson, 2004; Marton et al., 2000; Oluboyo et al., 2014)~~. The differential sieving continued for 36 hours before sieving of sedimentary wedges started again (Fig. 3). Basin 2b, in contrast, had an even thickness of 1 mm for the pre-kinematic layer (Fig. 3). Further sedimentation was only added to cover the exposed, reflective silicone to allow the monitoring system to work properly (~~. **~~Appendix~~** ~~Table A2). Thus, sieving rate on average in this silicone basin was very low.~~

~~3.~~6. ~~Experiment 3 investigates the translational domain development under a thin pre-kinematic layer and low sedimentation rate. Both Basin 3a and 3b had~~Model F has both pre-kinematic ~~layers of~~ layer (0.5 mm ~~thickness~~) and sedimentation rates ~~of~~ (0.5 mm per ~~12 hours~~sieving) reduced by a factor of two comparing to Model E (Fig. ~~3). However, differential loading was created in Basin 3a by~~ 3f). We only add three minibasins as differential loading in the upslope area, with similar geometr~~y~~ies to those ~~in Basin 2a (Fig. 3).~~of Model E (Fig. 3f).

The objective is testing minibasin behaviours with thinner thickness. Model F also serves as a comparison to Model 3 where no minibasin loading is introduced. The syn-kinematic differential sedimentation also continue~~d~~s for three sieving periods before wedge shaped syn-kinematic sedimentation ~~was~~is applied (Appendix Table ~~A2~~A1).

2.4 Experimental monitoring

We apply state-of-the art strain monitoring methods ~~based on~~using digital image correlation (DIC) to derive quantitative observational data from the experiments. The~~ evolving~~ model surface is monitored by a stereoscopic pair of two digital 12-bit monochrome CCD cameras with 29 mega pixels (LaVision Imager X-Lite 29M) at a time interval of 100 s (0.01 Hz frequency). We attach the cameras and ~~an ~~a light (LED) system to a frame moving with the base. Thereby only deformation with respect to the base is recorded, i.e. gravity gliding without interfering with the tilting motion. The recorded stereoscopic images are processed with ~~digital image correlation (~~DIC~~)~~ techniques which allows deriving the surface topography and full ~~3 ~~three-dimensional incremental surface velocity field with high accuracy ($\leqslant$ 0.1 ~~px~~mm) ~~(Adam et al., 2005). We use Davis Strainmaster 8 by LaVision software applying least square methods (LSM) algorithms.~~(Adam et al., 2005).

~~The DIC ~~We base our kinematic model analysis ~~yields quantitative deformation information of the experiment surfaces, such as ~~on incremental ~~and cumulative ~~horizontal ~~(~~downslope displacements (or velocity, Vx) reflecting gravitational sliding, and vertical displacements (or velocity, Vz~~), i.e.~~) reflecting subsidence and uplift~~.~~ associated with cover deformation and silicone flow. From the surface ~~velocities the incremental~~displacements, longitudinal strain (ε_{xx}) is derived. Moreover, ε_{xx} is extracted along the ~~symmetry~~centre axis of the ~~models (downslope) are derived (~~basins (downslope direction) at 1 hour intervals and displayed in the form of space-time plots, here referred to as strain ~~profile data).~~evolution (or strain rate) diagrams. DIC analysis allows us to quantitatively constrain and analy~~z~~se the structural and kinematic evolution of the model at high spatial (resulting vector spacing about 1-2 mm, at a vector accuracy of few tens of microns) and ~~sufficient ~~temporal resolution (100 seconds). ~~Digital image correlation ~~DIC data generated in this study ~~is~~are published open access in ~~Ge et al. (2019)~~.

3. Experimental observations and modelling results

~~To describe the model structural evolution both qualitatively and quantitatively, we visualize~~We use DIC-derived ~~data~~surface deformation data displayed as maps of surface incremental displacement (Vx and ~~strain, as well as space-time plots of~~ Vz) and longitudinal strain ~~profile data (i.e. strain evolution plots) in combination with cross sections of the finite models to demonstrate the temporal and spatial evolution of kinematic domains and individual structures. Representative~~(ε_{xx}). Incremental surface displacements and longitudinal strains from three intervals~~—~~: early, 25–36 ~~hours~~hour (7–9 Ma in nature), mid, 61–72 ~~hours~~hour (16–18 Ma in nature), and late, 109–120 ~~hours—~~hour (28–30 Ma in nature), that represent snaphots of the surface ~~geometry and evolution from early, mid and later stages~~deformation of the experiments (e.g. Fig. 4). ~~Fig. 4). The strain evolution plots~~As the tilting of the experiments lasts from 1–84 hour (1-21 Ma in nature), the early and mid stages show basin evolution during tilitng and the late stage represent basin status after tilting. The strain evolution diagrams visualize the surface strain rate evolution in the centre of each silicone basin through time ~~(e.g. Fig. 5a). The strain evolution plots~~and are tied to the cross sections showing the ~~exact location~~final structural geometry at the end of the ~~structures and their spatial and temporal evolution as seen at the model surface~~experiment (e.g. Fig. 5a).

3.1 ~~Experiment 1~~Model A

In ~~experiment 1~~Model A, after the first period of syn-kinematic sieving~~both silicone basins 1a and 1b are~~, the silicon basin is dominated by gravity gliding with upslope extension, mid-slope translation and downslope contraction (Fig. 4a–c).~~4). However,~~ In the early stage of ~~Basin 1a, where~~ the ~~pre-kinematic layer is 1 mm thick, an *c.*~~experiment (25–36 hour; 7–9 Ma in nature), a *c.* 10 cm (10 km in nature) wide belt with extensional grabens and diapirs occurs at the uppermost ~~edge of the slope.~~area of the slope (Fig. 4a). This extensional domain continues to expand downslope to the end of the experiment, reaching to over 20 cm wide (20 km in nature) (Figs 4b, c and 5a). Downdip, two significant thrusts and folds develop with an interval of *c.* 10 cm near the lowermost edge of the silicone basin (ε_{xx} in Fig. 4a). In the mid stage of the experiment (61–72 hour; 16–18 Ma in nature), the thrust belt expands both upslope and downslope with all thrusts being active in the late stage of the experiment (109–120 hour; 28–30 Ma in nature) (ε_{xx} in Fig. 5a). ~~In contrast, in Basin 1b, the cover layer~~ In the mid-slope, the translational domain occurs from the beginning of the experiment with *c.* 70 cm wide (70 km in nature), and gradually shrinks as the extensional and contractional domains expand (Fig. 5a). By the end of the experiment, the translational domain is *c.* 45 cm long (45 km in nature) (Fig. 5a). Overall, the model shows a clear domain partitioning from extension through translation to contraction, similar to the classic conceptual model of kinematic domains within passive margin salt basins (Fig. 1a).

3.2 Model B

In Model B, with a thicker, 5 mm thick pre-kinematic cover, the model surface remains largely undeformed in the early stage ~~as~~of the experiment (25–36 hour; 7–9 Ma in nature) with only a single extensional graben develop~~s~~ed at the upslope ~~tip~~edge of the basin, and no visually resolvable contractional structures ~~occur~~ in the downslope (ε_{xx} in Fig. ~~4a).~~

~~In Basin 1b,~~4d). However, the thick cove strata still drive the silicone flowing from the upslope to the downslope, leading to the uplift of the downslope area (Vz in Fig. 4b). Major deformation starts in the mid stage ~~when~~ (*c.* 60 hour; 15 Ma in nature) when normal faults occur in the upslope creating a *c.* 10 cm (10 km in nature) wide extensional domain (Fig. 4e). At the same time, a thrust belt T_{b1} occurs *c.* ~~10~~15 cm (15 km in nature) away from the ~~silicone basin tip in the~~ downslope ~~(ε_{xx} in~~ basin edge (Fig. 5b). ~~In the late stage,~~In the mid-slope, the translational domain occurs with *c.* 65 cm wide (65 km in nature) between the extensional and contractional domains (Fig. 5b). In the late stage of the experiment (109–120 hour; 28–30 Ma in nature), as the extensional domain slowly expands to *c.* 15 cm wide (15 km in nature), a frontal thrust T_{b2} occurs at the ~~tip~~downslope edge of the silicone basin (~~ε_{xx} in~~ Fig. 5b). However, as the front thrust T_{b2} is initiated, the early thrust T_{b1} gradually becomes inactive (Fig. 5b). ~~At the same time in Basin 1a, the thrust belt shifts~~The resultant translational domain of Model B is *c.* 55 cm wide (55 km in nature), larger than that of Model A (Fig. 5a and b).

3.3 Model C

Model C has a reduced pre-kinematic layer thickness (0.5 mm) as well as reduced syn-kinematic sedimentation (0.5 mm per 12 hours) compared to Model A, therefore the cover thickness of Model C is half as that of Model A (Fig. 3c). The domain evolution of Model C is similar to Model A, but with some important variations. The upslope extensional domain of Model C starts wider than Model A with *c.* 20 cm in width (20 km in nature), and expands gradually to be over 30 cm wide (30 km in nature) in the mid stage (61–72 hour; 16–18 Ma in nature) (Fig. 6a and b). The contractional domain initially starts with *c.* 10 cm wide (10 km in nature) near the downslope edge, but migrates upslope to *c.* 40 cm after 72 hours (18 Ma in nature). In the mid-slope, the translational domain occurs with *c.* 70 cm in width (70 km in nature) at early stage (25–36 hour; 7–9 Ma in nature), but diminishes continuously as both the extensional and contractional domains expand towards the ~~basin tip of the downslope as well as the upslope and both thrust belts keep active into the late stage (ε_{xx} in Fig.~~ mid-slope (Fig. 7a). By the end of the experiment, the translational domain is completely overprinted as the contraction reaches the extensional domain in the upslope, squeezing the early extensional structures (Fig. 7a).~~5a). Consequently, the contractional domain in Basin 1a is larger than that in Basin 1b at the end of the experiment (Fig. 5a and b). As both extensional domains of basins 1a and 1b are 20 cm long along dip direction, the resultant translational domain is smaller in Basin 1a (*c*. 40 cm) compared to that (50 cm) of Basin 1b (Fig. 5a and b). In short, both basins 1a and 1b show a clear domain partitioning from extension through translation to contraction, as described in the classic conceptual model (Fig. 1a).~~

3.4 Model D

Model D has the same pre-kinematic layer thickness (1 mm) as Model A, but no syn-kinematic sedimentation in the early stage and only negligible sedimentation afterwards (Appendix Table A1). The extensional structures are initiated across a *c*. 20 cm wide area (20 km in nature) in the upslope and expand to more than 40 cm wide (40 km in nature) in the mid stage (61–72 hour; 16–18 Ma in nature) (Figs 6d and 7b). Contractional structures occur across an area of *c*. 20 cm wide (20 km in nature) near the downslope edge of the basin (Fig. 7b). The contractional belt converges into an area of approximately 10 cm wide (10 km in nature) before the contraction migrates upslope after 72 hours (18 Ma in nature) (Figs 6f and 7b). The translational domain in the mid-slope occurs with *c*. 60 cm wide (60 km in nature) and shrinks to *c*. 40 cm wide in the mid stage (61–72 hour; 16–18 Ma in nature) (Fig. 7b). Due to the thin cover layer in the mid-slope (~ 1 mm), the migration of the contractional domain towards upslope causes short-wavelength (*c*. 2 ~~**Experiment 2**~~cm) folding in the translational domain in the late stage of the experiment (after 96 hours; 24 Ma in nature) (Figs 6f and 7b). At the end of the experiment, the contractional domain overlaps the extensional domain, causing squeezing of extensional diapirs and folding of the cover layer, overprinting the simple, undeformed translational domain (Fig. 7b).

~~In experiment 2, the two silicone basins 2a and 2b show~~3.5 Model E

Model E shows considerable differences in structural style and evolution compared to the other models (Models A–D), due to different sedimentation patterns~~.~~ (Fig. 3e). In ~~Basin 2a~~Model E, differential loading of the pre-kinematic ~~layer~~ and early syn-kinematic sieving ~~results~~within 8 minibasins result in a basin-wide imprint of minibasin~~s~~ downbuilding~~, as shown by~~. The differential loading process is most prominent on the subsidence pattern during the early stage where ~~strings of~~ thicker ~~pre-kinematic layer~~minibasin areas subside stronger than ~~intervened regions forming minibasins~~the intervening areas of diapirs (Vz in Fig. ~~6a~~8a). However, minibasin downbuilding only dominates the deformation for a very short period of ~~about~~ 1 to 2 hours (0.25–0.5 Ma), during which time the minibasins ~~extend~~ and ~~areas~~diapirs in between are ~~affected by~~

~~diapirism~~areas of extension and contraction respectively, with no sign of a translational domain (Fig. ~~7a~~9a). Shortly afterwards, gravity gliding takes over as the extension ~~dominated~~and contraction dominate the upslope and ~~contraction dominated the~~ downslope ~~(Fig. 7a~~respectively, forming a *c.* 10 cm wide (10 km in nature) extensional domain and a *c.* 10 cm wide contractional domain (Figs 8b and 9a). During the transition, the ~~minibasin area (apart from Minibasin 1) becomes a shadow zone of~~ deformation ~~and transfer strain passively while the~~ concentrates on diapirs ~~start to accommodate~~, and little deformation is observed within the minibasins (Fig. ~~7~~9c). In the mid and late stages~~, Basin 2a~~ of the experiment, Model E develops similar surface pattern to ~~the basins in the experiment 1 with clear domains of extension, translation and contraction (Fig. 7a). In contrast, Basin 2b has a different structural style and basin evolution comparing to Basin 2a. Since Basin 2b has the same pre-kinematic layer thickness as in Basin 1b, the evolution of kinematic domain partitioning from early to mid stage are similar in both experiments. However, in Basin 2b, as there is no syn-kinematic sedimentation in the early stage and only minimum sedimentation afterwards (Appendix Table A2), extensional structures are initiated in a wider area of c. 30 cm along dip and grow even larger to more than 40 cm in late stage (Figs 6a and 7b). Contractional structures occur in an area of c. 20 cm along dip near the tip of the downslope of the Basin 2b (Fig. 7b). The contractional belt converges into an area of approximately 10 cm wide before the contraction migrates upslope in the later stage (Figs 6c and 7b). Due to the thin cover layer in the mid-slope (~ 1 mm), the migration of the contractional domain upslope causes short-wavelength folding in the translational domain (Fig. 7b). At the end of the experiment, the contractional domain overlaps with previous extensional domain, causing squeezing of extensional diapirs and deformation of the cover layer in the former translational domain (Fig. 7b).~~Model A with downslope contraction migrating towards upslope (Fig. 9a).

3.~~3 Experiment 3~~6 Model F

~~In experiment 3, both silicone basins 3a and 3b have a~~Comparing to Model E, Model F has reduced pre-kinematic layer ~~of 0.5 mm~~thickness and ~~a~~ syn-~~-~~kinematic sedimentation ~~rate of 0.5 mm/12 hours. As a result, the structural evolution of both basins share many similarities (Fig. 8). The~~and only ~~difference is that~~ three minibasins ~~are created~~ in the upslope ~~of the pre-kinematic layer in Basin 3a while the pre-kinematic layer has even thickness in Basin 3b. Sieving of these minibasins continues for three periods (Appendix Table A2).~~

~~In Basin 3a,~~area (Fig. 3f). The differential loading ~~dominates~~in the upslope ~~deformation briefly~~area in the first 1–2 hours of ~~the experiment (Fig.10a), similar to what~~Model E is also observed in ~~Basin 2a (Fig. 7c).~~Model F. However, ~~since~~because the minibasins are located only in the upslope, more proximal area ~~of Basin 3a~~ and the ~~sieving~~sedimentation rate is half ~~compared to Basin 2a~~that of Model E, the imprint of minibasin downbuilding on the structural evolution is less significant comparing to ~~Basin 2a.~~Model E (Fig. 8d). For example, the ~~diapir~~early stage minibasins and diapirs formation preserved ~~between the minibasins 2 and 3~~ in the cross section ~~has limited height and is~~ are much smaller than similar structures in Model E (Fig. 9a). Moreover, as minibasins only form in the proximal part of the mid-slope, a translational domain occurs in the distal part of the mid-slope with *c*. 40 cm in width (40 km in nature) (Fig. 9b). ~~diapirs in Basin 2a (Fig. 9a).~~

~~Importantly, the differential loading in Basin 3a also influences the development of extensional structures. For example, the extensional grabens develop earlier in Basin 3a than those in Basin 3b (Fig. 9a and b). Similarly, the~~ From 48 hours (12 Ma in nature) and onwards, the extensional domain dominates the upslope and continues to expand to > 30 cm wide (30 km in nature) by the end of the experiment (Fig. 9b). The downslope contractional domain is *c*. 15 cm wide (15 km in nature) initially, and expands to *c*. 60 cm wide (45 km in nature) due to upslope migration of ~~the contractional domain also starts early in Basin 3a, as many small wavelength folds occur in the former translational domain at 60 hours and afterward (Figs 8b and 9a). In contrast, the upslope migration of contraction occurs after 84 hours in Basin 3b (Figs 8c and~~contraction (Fig. 9b). By the end of the experiment, the ~~9b). By the end of the experiment, in both basins 3a and 3b, upslope migrated~~ contractional structures interfere with early extensional structures, resulting in ~~a deformed~~an overprinted translational domain (Fig. ~~9a and b~~9b).

4. Discussion

We used basin-scale sandbox analogue modelling to study the first order controls on origination, development and ~~destruction~~overprinting of the translational domain in salt-bearing passive margin basins where the thin-skinned salt tectonics dominates the structural and stratigraphic evolution. Based on the analysis of temporal and spatial evolution of ~~kinematic domains and~~ individual structures~~,~~ and kinematic domains of extension, translation and contraction; we identify the translational domain as a transient feature ~~destructed~~. It is modified by two potential mechanisms: i) migration of extensional and contractional domains into a previous undeformed translational domain; ii) differential loading by sedimentation into minibasins that triggers salt-related structures, such as diapirs, from the beginning of basin evolution, therefore, prevent~~s~~ing the formation of a tectonically stable translational domain.

4.1 ~~Control~~Influences of pre- and syn-kinematic layer thickness ~~and sedimentation rate~~ on ~~formation of a~~the translational domain

Our modelling results are in good agreement with previous works where a translational domain is evident when a relatively thick and continuous ~~homogeneous pre-kinematic layer exists. Translational domains have been observed~~pre-kinematic layer exists (e.g. Dooley et al., 2018; Fort et al., 2004a). Translational domains have been observed in other experiments with a pre-kinematic layer of even thickness in the order of 3–10 mm (300 to 1000 meters in nature) (Adam et al., 2012a; Adam and Krezsek, 2012; Fort et al., 2004a). Similar observations are ~~derived from this study~~made in Model A and B where about 50% of the basin length is occupied by the translational domains ~~within basins 1a and 1b~~ (Fig. 5). As noted by ~~Brun and Fort (2012)~~, the cover layer needs to be thick and strong enough to transfer the strain without deforming internally. In many analogue models, the total thickness of pre- and syn-kinematic layers is usually on the order of a few centimetres (e.g. Adam et al., 2012a; Fort et al., 2004a), which equals to a few kilometres in nature using a similar geometric scaling factor from this study (1 cm in model is 1 km in nature). ~~According to~~Results from our study~~,~~ suggest that a 1 mm thick pre-kinematic layer and 2-3 mm ~~sediment from~~thick syn-kinematic sedimentation (few hundreds of meters if scaled to nature) seems strong enough to form a stable translational domain from beginning to end, such as ~~in Basin 1a (Fig. 5a).~~ the one (*c.* 45 cm wide; 45 km in nature) in Model A (Figs 5a). With a thicker cover, such as Model B (5 mm pre-kinematic layer), the translational domain gets even larger (*c.* 55 cm wide; 55 km in nature) due to stronger cover (Fig. 5b).

4.2 ~~Translational domain destruction~~Overprinting the translational domains by deformation migration

Our study shows that a very thin supra-salt cover, combining a thin pre-kinematic layer with a very low sedimentation rate, allows the downslope migration of extensional domains and upslope migration of contractional domains, which ultimately leads to the ~~destruction~~overprint of the translational domain (~~Fig. 10a~~Figs 7a and10a). Specifically, in Model C, when the pre-kinematic layer is only 0.5 mm in the models (50 m in nature) and syn-kinematic sedimentation is 1 mm/day (about 17 m per Ma in nature), the translational domain can be ~~destructed~~overprinted by the migration of extension and contraction towards the ~~basin centre~~mid-slope (Fig. ~~9a~~7a and b). This contrast to Model A and B (Fig. 5), as well as other studies with thick pre- and syn-kinematic layers (e.g. Adam et al., 2012a; Brun and Fort, 2004; Fort et al., 2004a), where the undeformed translation domains are either fully or partially preserved, even under the influence of upslope migration of contraction. However, the simulated sedimentation rate of ~~about~~ 17 m/Ma in nature is extremely low comparing to natural salt basins where the typical sedimentation rate is ~~in the order of~~> 100 m/ Ma (Adam et al., 2012a; Adam and Krezsek, 2012). In general, such low sedimentation rates are more compatible with typical hemiplegic sedimentation rates of 2–20 m/Ma ~~(Stow et al., 2001).~~(Stow et al., 2001). This implies that our models including a very thin pre-kinematic layer and a very low sedimentation rate may ~~be~~ not ~~archetypical~~be typical of passive margin salt basins ~~where the terrigenous~~with high terrestrial input ~~is generally significant~~ (e.g. Fig. 1b and c). ~~Therefore, the first proposed mechanism for translational domain destruction by deformation migration might be active only in special geological settings where sediment supply is limited.~~

In some cases, when margin tilting is modified due to basement tectonics, deformation migration may also occur even with a thick supra-salt cover. A good example is the Kwanza Basin, Angola, where a major Miocene sub-salt uplift of the basin in the upslope area leads to a reactivation of basin-wide thin-skinned deformation (e.g. Hudec and Jackson, 2004). The uplifted area has average cover thickness over 2 km, yet shows evidence of extension migrating towards both upslope and downslope (Hudec and Jackson, 2004; their fig. 9).

4.3 Overprinting the translational domain ~~destruction~~ by differential loading

~~A more plausible mechanism for translational domain destruction suggested by our~~ The results of the experiments ~~is~~documented here suggest that differential loading in the mid-slope ~~along with the occurrence of minibasins and diapirs~~ is a viable mechanism for overprinting the translational domain (Fig. 10b). ~~In experiment 2, the~~ Basin-wide differential loading ~~was~~is applied in ~~Basin 2a~~Model E (Fig. ~~7a~~9a), which result~~ed~~s in the formation of minibasins and diapirs~~.~~ in the mid-slope. Even though the differential loading only dominate~~d~~s the basin for a short, early period (roughly 1.5 hours in the model or 0.~~375~~4 Ma in ~~the~~ nature), the translational domain ~~was~~is overprinted completely ~~deformed.~~during the time. Although the pattern of differential loading is idealized in the experiments~~, similar sedimentation patterns might persist~~ as a series of minibasins, variation of sediment deposition occurs in nature as ~~natural sedimentary systems deliver variable~~ sediment supply through ~~alternating fairways resulting~~discrete sediment routing systems results in different sediment thicknesses across the basin. For example, restorations of the earliest stratigraphic units in passive margin salt basins have always been patchy with ~~various thicknesses in~~marked thickness variations between different locations (e.g. Adam et al., 2012b; Hudec and Jackson, 2004; Marton et al., 2000). Moreover, numerical simulation has demonstrated that such patchy pattern of ~~minibasins intervened~~minibasin depocentres, separated by salt diapirs can be simply formed by differential loading alone ~~(Peel, 2014)~~.

Since the scenario of early differential loading is more realistic than a thick and uniform supra-salt cover, the strain transfer from upslope extension to downslope contraction may not ~~be through~~need a simple translational domain as current models suggest (Figs 1a~~, 10c~~ and ~~d~~10c). The thick and strong minibasins and intervened weak diapirs form heterogeneit~~y~~ies within the supra-salt sediment cover and complicate the pattern of strain transfer. For example, the minibasins in ~~the Basin 2a were~~Model E are passively translated ~~individually~~ and the diapirs in between accommodate~~d~~ the deformation ~~in the early stage~~ (Figs ~~7c~~9c and 10d). In this way, the deformation ~~partially transfers from the upslope extension to the downslope contraction but~~ is ~~partially accommodated~~transferred by a combination of minibasin translation and diapir ~~squeezing~~widening (extension) and shortening (contraction) in the mid-slope (Fig. 10d). ~~A translational domain therefore is not necessary~~However, the strike orientations of minibasins and associated diapirs in this study are all perpendicular to the orientation of thin-skinned deformation. In reality, the diapirs with various orientations may connect to ~~be present~~each other forming a network, as has been observed in the northern Gulf of Mexico (e.g. Rowan and Vendeville, 2006). Consequently, during ~~the whole evolution of the passive margin salt basins~~thin-skinned deformation, the associated strain distribution of diapirs may be more complex than our models suggest.

4.4 Alternative mechanisms for overprinting translation ~~domain destruction~~domains

Other mechanisms may also be responsible for the ~~destruction~~absence or ~~nonexistence~~overprinting of a well-defined translational domain. One potential mechanism is ~~sub-salt~~a step or relief of the base of the salt associated with early tectonic activity ~~in passive margin salt basins~~(e.g. rift-related topography) (Jackson and Hudec, 2005; Pichel et al., 2018). Analogue models with sub-salt steps/relief have demonstrated that these basement structures can cause strain localization ~~within~~of the supra-salt cover strata around them therefore complicating the structural style and ~~deforming~~overprinting the translational domain (e.g. Dooley et al., 2017; Dooley et al., 2018; Ferrer et al., 2017; Gaullier et al., 1993).

~~Moreover,~~ Progradational sedimentary wedges can also ~~prevent~~cause overprinting the translational domain~~ from forming.~~. As the sedimentary wedges ~~progressively~~ generate extension and contraction in the upslope and downslope areas within the wedges, progradation of the sedimentary wedges bring the associated extensional and contractional domains to move ~~basinwards~~forward. Consequently, early formed ~~contractional structures~~ translational domains in the middle of the sedimentary wedge are superimposed by late, forward-moving extensional structures~~, completely destroying the translational domain~~ (Brun and Fort, 2011; McClay et al., 1998; Vendeville, 2005).

~~Although the sedimentary wedge is~~Furthermore, sediment progradation direction and rate may also ~~one type of differential loading, the absence of tilting makes the system very different from the ones presented in this study. Future research therefore is needed to fully understand the influences of sub-salt structures and progradational wedges on~~have variations across the ~~development and destruction~~margin and thus further complex the process of translational ~~domains.~~domain overprinting (e.g. Brun and Fort, 2018; Fort et al., 2004b).

5. Conclusions

Sandbox analogue modelling analy~~z~~sed by 4D digital image correlation (DIC) allow~~ed~~s a thorough and precise analysis of the evolution and kinematic domain partitioning ~~, as well as structural evolution~~ of ~~a~~ passive margin salt basins under different combination of pre- and syn-kinematic sedimentation ~~patterns.~~

. Experiments with uniform pre-kinematic cover thickness show a typical domain partition of upslope extension compensated by downslope contraction with an intermediate ~~translational~~ domain~~.~~

of translation. Under such circumstances, even very thin (1 mm or 100 m in nature) pre-kinematic cover ~~was~~is sufficient to generate ~~the~~a translational domain~~. For a thick~~, and it becomes wider with a thicker supra-salt cover~~, the translational domain persisted until the end of the experiment.~~

. We identifi~~ed~~y two scenarios in which the translational domain ~~can be considered~~is only a transient feature ~~destructed~~ during ~~the course of an experiment. First~~basin evolution and becomes progressively overprinted and destroyed. Firstly, when the initial cover layer is thin and sedimentation rate is low, upslope migration of the contractional domain ~~completely~~ overprints the translational domain. Secondly, when early differential sediment loading ~~is applied~~occurs in the mid-slope area, formation of minibasins ~~intervened~~separated by diapirs ~~in the mid-slope destructs~~also overprint the translational domain.

A comparison between analogue models and natural ~~cases~~examples of passive margin salt basins suggests that an undeformed translational domain, as seen in analogue models~~ rarely~~, occurs rarely in nature. This ~~seems~~is because the sediment deposition from natural sedimentary systems tends to ~~be related~~ have thickness variations and is unlikely to ~~the general implementation of~~ form a thick, mechanically stable (or rigid and undeformable) supra-salt cover layer as that in analogue models~~ neglecting the subtle initial thickness variations likely present in natural sedimentary systems.~~. Low sedimentation ~~rate~~rates are required ~~for the destruction of~~to overprint the translational domain through migration of the extensional and contractional domains ~~as suggested by~~. Our study suggests this is ~~also~~ rare in natural passive margins~~.~~ due to high clastic sediment input. Instead, a more viable mechanism in nature is differential loading with initial thickness variations ~~within~~of the supra-salt cover ~~creating differential loadingand furthermore causing~~ that causes overprinting of the translational domain ~~destruction~~ through the formation of ~~mid-slope~~ minibasins and diapirs ~~seems to be a more viable mechanism in nature.~~. Other factors, such as progradation of sedimentary wedges and sub-salt related deformation or relief, can also be responsible for modifying the translational domain through domain migration and perturbing the strain distribution in the supra-salt cover strata.

Data availability. The experimental data, along with analysis code, are available on the GFZ repository (Ge et al., 2019).

Author contributions. ZG, MR and RG designed the experiments. ZG~~, MR~~ and MW ran the experiments. ZG, MR and MW processed the data and did the strain analysis. All authors contributed to the writing of the manuscript.

Competing interests. The authors declare no conflict of interest.

Acknowledgement

The project was supported by E.ON Stipendienfonds and 2018 TNA program of EPOS' Thematic Core Service Multi-scale Laboratories. ZG would like to thank Equinor for sponsorsing his postdoc at University of Bergen. We thank Frank Neumann and Thomas Ziegenhagen for construction of the experimental device as well as the whole laboratory team for scientific assistance. Danielle Howlett is thanked for remarks on an early version of the paper. Frank Zwaan and Tim Dooley are thanked for their constructive reviews that improve the quality and clarity of the manuscript. We also thank editor Mark Allen for editing suggestions. We thank GFZ Data Services for making the data underlying this study open accessible (Ge et al., 2019; Warsitzka et al., 2019).

References

Adam, J., Ge, Z., and Sanchez, M.: Post-rift salt tectonic evolution and key control factors of the Jequitinhonha deepwater fold belt, central Brazil passive margin: Insights from scaled physical experiments, Mar. Pet. Geol., 37, 70–100, 2012a.

Adam, J., Ge, Z., and Sanchez, M.: Salt-structural styles and kinematic evolution of the Jequitinhonha deepwater fold belt, central Brazil passive margin, Mar. Pet. Geol., 37, 101–120, 2012b.
Adam, J. and Krezsek, C.: Basin-scale salt tectonic processes of the Laurentian Basin, Eastern Canada: insights from integrated regional 2D seismic interpretation and 4D physical experiments, Geological Society, London, Special Publications, 363, 331–360, 2012.
Adam, J., Urai, J. L., Wieneke, B., Oncken, O., Pfeiffer, K., Kukowski, N., Lohrmann, J., Hoth, S., van der Zee, W., and Schmatz, J.: Shear localisation and strain distribution during tectonic faulting—new insights from granular-flow experiments and high-resolution optical image correlation techniques, J. Struct. Geol., 27, 283–301, 2005.
Allen, J. and Beaumont, C.: Impact of inconsistent density scaling on physical analogue models of continental margin scale salt tectonics, Journal of Geophysical Research: Solid Earth, 117, 2012.
Brun, J.-P. and Fort, X.: Compressional salt tectonics (Angolan margin), Tectonophysics, 382, 129-150, 2004.
Brun, J.-P. and Fort, X.: Growth of Continental Shelves at Salt Margins, Frontiers in Earth Science, 6, 2018.
Brun, J.-P. and Fort, X.: Salt tectonics at passive margins: Geology versus models, Mar. Pet. Geol., 28, 1123–1145, 2011.
Brun, J.-P. and Fort, X.: Salt tectonics at passive margins: geology versus models–Reply, Mar. Pet. Geol., 37, 195–208, 2012.
Costa, E. and Vendeville, B. C.: Experimental insights on the geometry and kinematics of fold-and-thrust belts above weak, viscous evaporitic décollement, J. Struct. Geol., 24, 1729–1739, 2002.
Cramez, C. and Jackson, M. P. A.: Superposed deformation straddling the continental-oceanic transition in deep-water Angola, Mar. Pet. Geol., 17, 1095–1109, 2000.
Dooley, T. P., Hudec, M. R., Carruthers, D., Jackson, M. P. A., and Luo, G.: The effects of base-salt relief on salt flow and suprasalt deformation patterns — Part 1: Flow across simple steps in the base of salt, Interpretation, 5, SD1vSD23, 2017.
Dooley, T. P., Hudec, M. R., Pichel, L. M., and Jackson, M. P. A.: The impact of base-salt relief on salt flow and suprasalt deformation patterns at the autochthonous, paraautochthonous and allochthonous level: insights from physical models, Geological Society, London, Special Publications, 476, 2018.
Dooley, T. P., Jackson, M. P. A., and Hudec, M. R.: Initiation and growth of salt-based thrust belts on passive margins: results from physical models, Basin Res., 19, 165–177, 2007.
Ferrer, O., Gratacós, O., Roca, E., and Muñoz, J. A.: Modeling the interaction between presalt seamounts and gravitational failure in salt-bearing passive margins: The Messinian case in the northwestern Mediterranean Basin, Interpretation, 5, SD99-SD117, 2017.
Fort, X., Brun, J.-P., and Chauvel, F.: Salt tectonics on the Angolan margin, synsedimentary deformation processes, AAPG Bull., 88, 1523–1544, 2004a.
Fort, X., Brun, J. P., and Chauvel, F.: Contraction induced by block rotation above salt (Angolan margin), Mar. Pet. Geol., 21, 1281-1294, 2004b.
Gaullier, V., Brun, J. P., Guerin, G., and Lecanu, H.: Raft tectonics: the effects of residual topography below a salt de´collement, Tectonophysics, 228, 363-381, 1993.
Ge, H., Jackson, M. P. A., and Vendeville, B. C.: Kinematics and dynamics of salt tectonics driven by progradation, AAPG Bull., 81, 398-423, 1997.
Ge, Z., Rosenau, M., Warsitzka, M., Rudolf, M., and Gawthorpe, R. L.: Digital image correlation data from analogue modeling experiments addressing mechanisms of destructing translational domains in passive margin salt basins. GFZ Data Services, http://doi.org/10.5880/GFZ.4.1.2019.001, 2019.
Gemmer, L., Beaumont, C., and Ings, S. J.: Dynamic modelling of passive margin salt tectonics: effects of water loading, sediment properties and sedimentation patterns, Basin Res., 17, 383–402, 2005.
Gradmann, S., Hübscher, C., Ben-Avraham, Z., Gajewski, D., and Netzeband, G.: Salt tectonics off northern Israel, Mar. Pet. Geol., 22, 597–611, 2005.
Gvirtzman, Z., Reshef, M., Buch-Leviatan, O., Groves-Gidney, G., Karcz, Z., Makovsky, Y., and Ben-Avraham, Z.: Bathymetry of the Levant basin: interaction of salt-tectonics and surficial mass movements, Mar. Geol., 360, 25–39, 2015.
Hoshino, K., Koide, H., Inami, K., Iwamura, S., and Mitsui, S.: Mechanical Properties of Tertiary Sedimentary Rocks under High Confining Pressure, Geological Survey of Japan, Kawasaki, Report, 244, 1972.

Hubbert, M. K.: Theory of scale models as applied to the study of geologic structures, Bull. Geol. Soc. Am., 48, 1459–1520, 1937.
Hudec, M. R. and Jackson, M. P. A.: Interaction between spreading salt canopies and their peripheral thrust systems, J. Struct. Geol., 31, 1114–1129, 2009.
Hudec, M. R. and Jackson, M. P. A.: Regional restoration across the Kwanza Basin, Angola: Salt tectonics triggered by repeated uplift of a metastable passive margin, AAPG Bull., 88, 971–990, 2004.
Jackson, M. P. A. and Hudec, M. R.: Stratigraphic record of translation down ramps in a passive-margin salt detachment, J. Struct. Geol., 27, 889–911, 2005.
Jackson, M. P. A. and Vendeville, B. C.: Regional extension as a geologic trigger for diapirism, Geol. Soc. Am. Bull., 106, 57-73, 1994.
Jaeger, J. C. and Cook, N. G. W.: Fundamentals of rock mechanics. Methuen & Co Ltd., London, 1969.
Koyi, H.: The shaping of salt diapirs, J. Struct. Geol., 20, 321–338, 1998.
Krézsek, C., Adam, J., and Grujic, D.: Mechanics of fault and expulsion rollover systems developed on passive margins detached on salt: insights from analogue modelling and optical strain monitoring, Geological Society, London, Special Publications, 292, 103–121, 2007.
Lallemand, S. E., Schnürle, P., and Malavieille, J.: Coulomb theory applied to accretionary and nonaccretionary wedges: Possible causes for tectonic erosion and/or frontal accretion, Journal of Geophysical Research: Solid Earth, 99, 12033-12055, 1994.
Marton, G., Tari, G. C., and Lehmann, C. T.: Evolution of the Angolan Passive Margin, West Africa, With Emphasis on Post ‐ Salt Structural Styles, Atlantic rifts and continental margins, 2000. 129–149, 2000.
Masrouhi, A., Bellier, O., Koyi, H., Vila, J.-M., and Ghanmi, M.: The evolution of the Lansarine–Baouala salt canopy in the North African Cretaceous passive margin in Tunisia, Geol. Mag., 150, 835–861, 2013.
Mauduit, T. and Brun, J. P.: Growth fault/rollover systems: birth, growth, and decay, Journal of Geophysical Research: Solid Earth, 103, 18119–18136, 1998.
Mauduit, T., Guerin, G., Brun, J.-P., and Lecanu, H. J. J. o. S. G.: Raft tectonics: the effects of basal slope angle and sedimentation rate on progressive extension, 19, 1219-1230, 1997.
McClay, K. R., Dooley, T., and Lewis, G.: Analog modeling of progradational delta systems, Geology, 26, 771–774, 1998.
Modica, C. J. and Brush, E. R.: Postrift sequence stratigraphy, paleogeography, and fill history of the deep-water Santos Basin, offshore southeast Brazil, AAPG Bull., 88, 923–945, 2004.
Oluboyo, A. P., Gawthorpe, R. L., Bakke, K., and Hadler ‐ Jacobsen, F.: Salt tectonic controls on deep ‐ water turbidite depositional systems: Miocene, southwestern Lower Congo Basin, offshore Angola, Basin Res., 26, 597-620, 2014.
Peel, F. J.: How do salt withdrawal minibasins form? Insights from forward modelling, and implications for hydrocarbon migration, Tectonophysics, 630, 222–235, 2014.
Pichel, L. M., Peel, F., Jackson, C. A. L., and Huuse, M.: Geometry and kinematics of salt-detached ramp syncline basins, J. Struct. Geol., 115, 208–230, 2018.
Ramberg, H.: Gravity, deformation, and the earth's crust: In theory, experiments, and geological application, Academic press, 1981.
Rowan, M. G.: Passive-margin salt basins: hyperextension, evaporite deposition, and salt tectonics, Basin Res., 26, 154–182, 2014.
Rowan, M. G., Peel, F. J., and Vendeville, B. C.: Gravity-driven fold belts on passive margins, AAPG Mem., 2004. 157–182, 2004.
Rowan, M. G. and Vendeville, B. C.: Foldbelts with early salt withdrawal and diapirism: Physical model and examples from the northern Gulf of Mexico and the Flinders Ranges, Australia, Mar. Pet. Geol., 23, 871–891, 2006.
Rudolf, M., Boutelier, D., Rosenau, M., Schreurs, G., and Oncken, O.: Rheological benchmark of silicone oils used for analog modeling of short-and long-term lithospheric deformation, Tectonophysics, 684, 12–22, 2016.
Schellart, W. P.: Analogue modelling of large-scale tectonic processes: an introduction. In: Analogue modelling of large-scale tectonic processes, Schellart, W. P. and Passchier, C. (Eds.), Journal of Virtual Explorer, 2002.
Stow, D. A. V., Huc, A. Y., and Bertrand, P.: Depositional processes of black shales in deep water, Mar. Pet. Geol., 18, 491–498, 2001.

Tari, G., Molnar, J., and Ashton, P.: Examples of salt tectonics from West Africa: a comparative approach, Geological Society, London, Special Publications, 207, 85-104, 2003.
Vendeville, B. C.: Salt tectonics driven by sediment progradation: Part I—Mechanics and kinematics, AAPG Bull., 89, 1071-1079, 2005.
Vendeville, B. C. and Jackson, M. P. A.: The fall of diapirs during thin-skinned extension, Mar. Pet. Geol., 9, 354–371, 1992a.
Vendeville, B. C. and Jackson, M. P. A.: The rise of diapirs during thin-skinned extension, Mar. Pet. Geol., 9, 331–354, 1992b.
Warsitzka, M., Ge, Z., Schönebeck, J.-M., Pohlenz, A., and Kukowski, N.: Ring-shear test data of foam glass beads used for analogue experiments in the Helmholtz Laboratory for Tectonic Modelling (HelTec) at the GFZ German Research Centre for Geosciences in Potsdam and the Institute of Geosciences, Friedrich Schiller University Jena. GFZ Data Services, http://doi.org/10.5880/GFZ.4.1.2019.002, 2019.
Warsitzka, M., Kley, J., and Kukowski, N.: Analogue experiments of salt flow and pillow growth due to basement faulting and differential loading, Solid Earth, 6, 9–31, 2015.
Weijermars, R., Jackson, M. P. A., and Vendeville, B.: Rheological and tectonic modeling of salt provinces, Tectonophysics, 217, 143–174, 1993.
Weinberger, R., Lyakhovsky, V., Baer, G., and Begin, Z. B.: Mechanical modeling and InSAR measurements of Mount Sedom uplift, Dead Sea basin: Implications for effective viscosity of rock salt, Geochem. Geophys. Geosyst., 7, 1–20, 2006.
Withjack, M. O. and Callaway, S.: Active normal faulting beneath a salt layer: an experimental study of deformation patterns in the cover sequence, AAPG Bull., 84, 627–651, 2000.

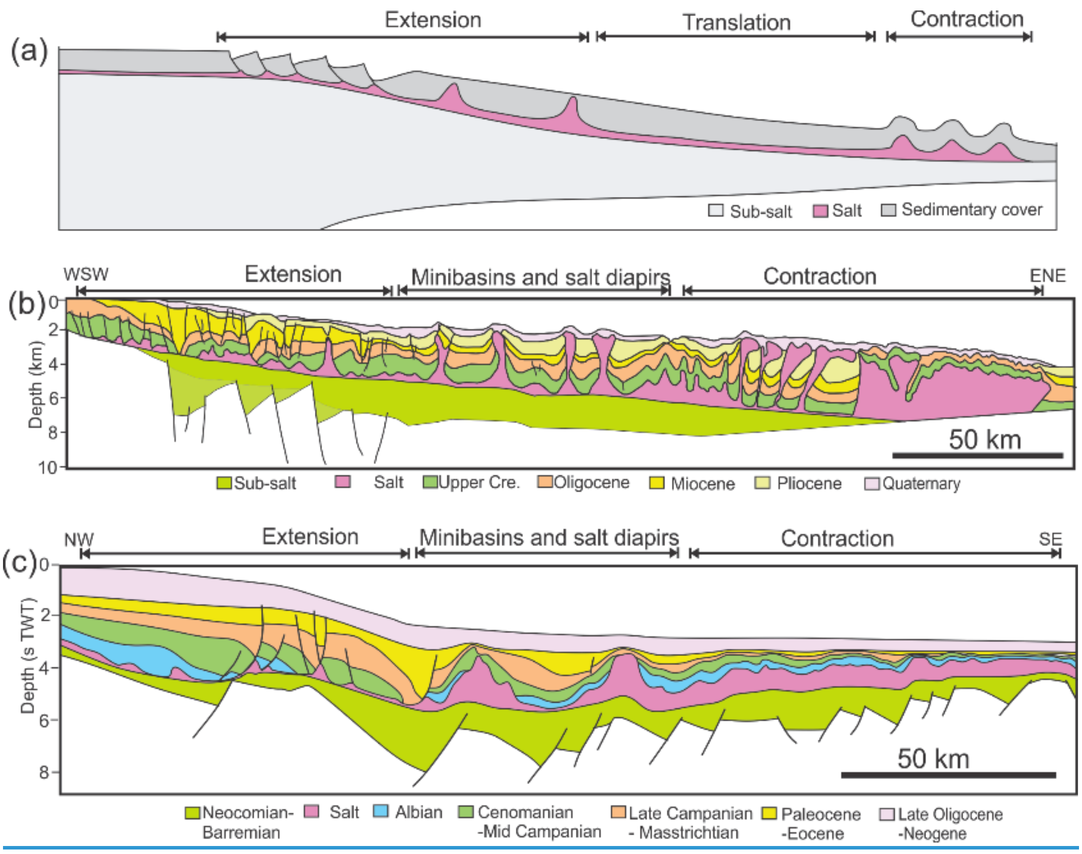

Figure 1. (a) Simplified cross section illustrating the kinematic domains and structural styles in a typical passive margin salt basin (modified after Rowan et al., 2004; Brun and Fort, 2011). (b) Regional interpreted seismic profile crossing the Lower Congo Basin (modified after Marton et al., 2000). Note the minibasins and diapirs in the mid-slope. (~~b~~c) Regional interpreted seismic profile crossing the Central Santos Basin (modified after Modica and Brush, 2004). Note the large minibasins and diapirs in the mid-slope area.

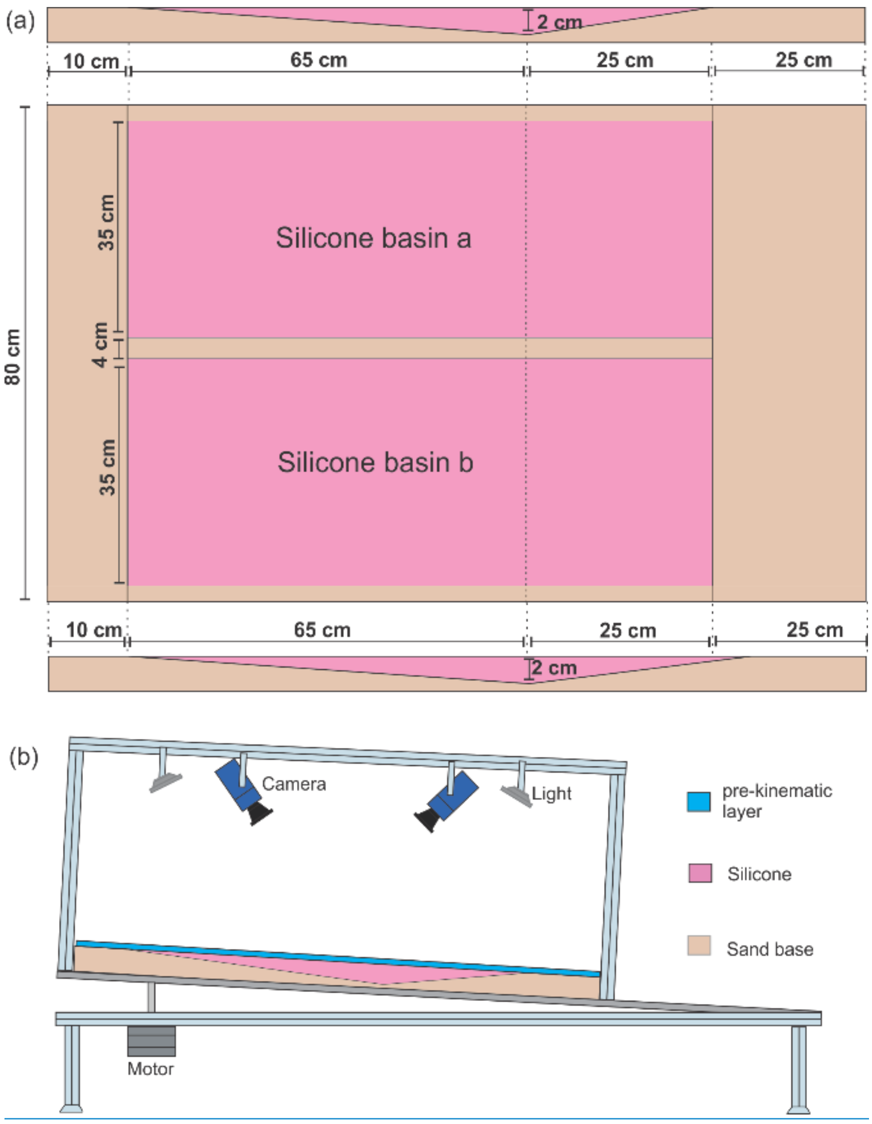

Figure. 2. Experimental setup and sketch of the apparatus. (a) Experimental setup ~~of the~~including two identical silicone basins~~.~~ in each experimental run. The double wedge shape of the silicone basin is 2 cm at its ~~thickest. (a~~deepest. (b) 2D sketch of the experimental setup. The cameras are attached to the tilting basal plate ~~pushed~~lifted by ~~the~~a stepper motor~~ beneath~~.

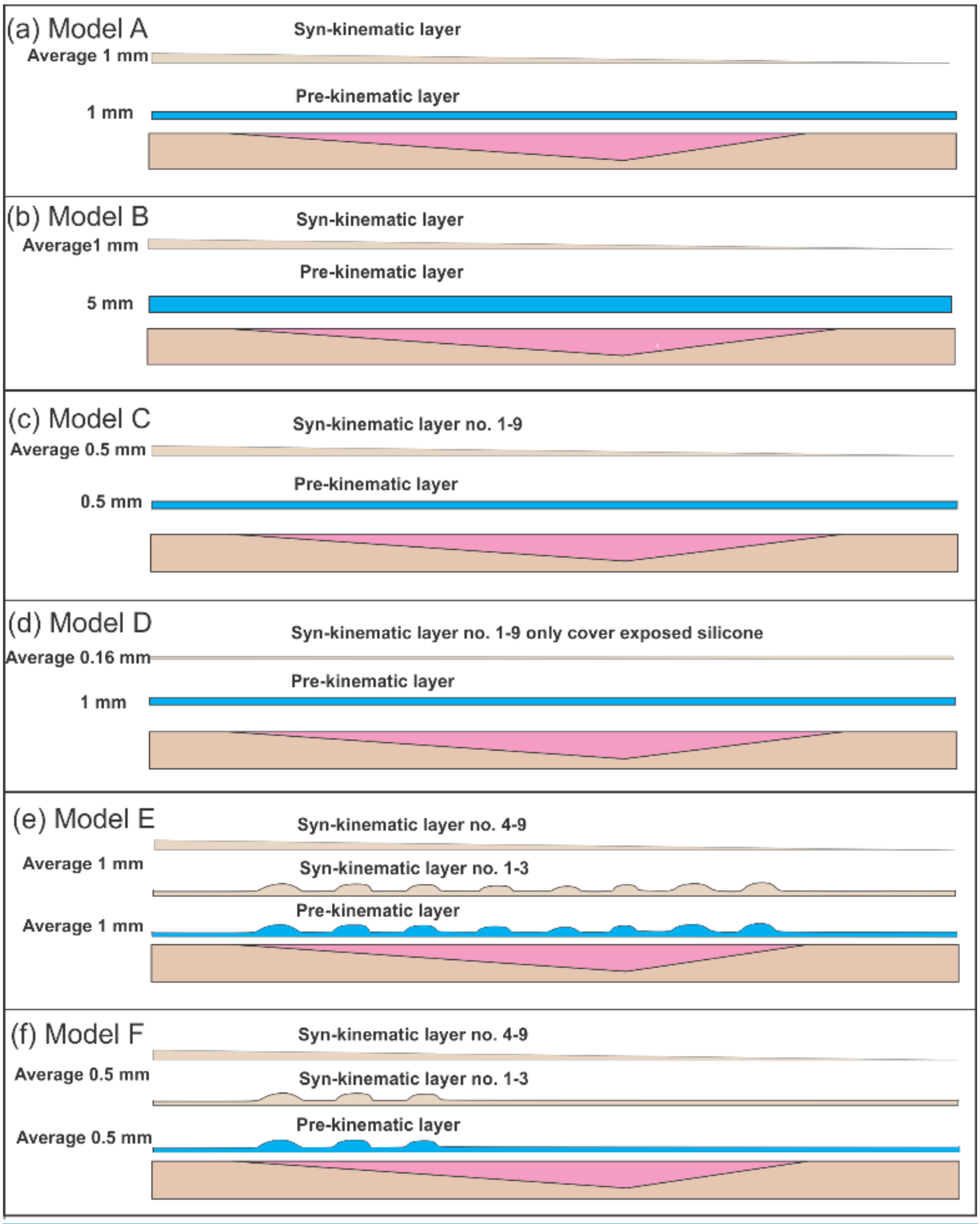

Figure. 3. Depositional scenarios for ~~all~~ six ~~silicone basins~~models of the three experiments. The blue layers are pre-kinematic ~~layer~~ and brown layers are syn-kinematic. Note the minibasin ~~shape associates~~shapes associate with differential loading in ~~basins 2a~~Model E and ~~3a~~F. The syn-sedimentation thickness is in average as they are ~~actually~~ in wedge shape.

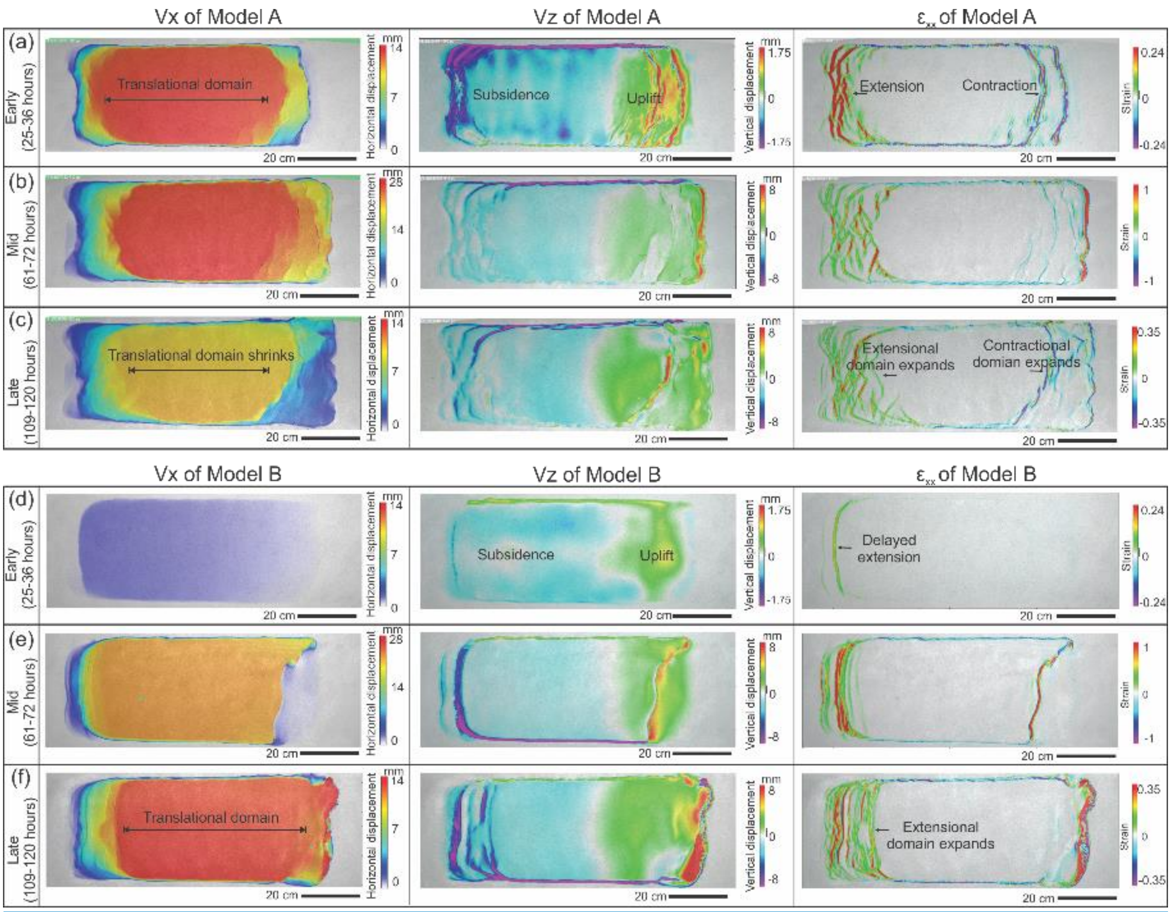

Figure 4. (a–c) Map view of ~~finite~~incremental horizontal and vertical displacement (Vx, Vz) and strain pattern (ε_{xx}) derived from 3D DIC strain data of ~~experiment 1~~Model A from the (a) early (25–36 hours), (b) mid (61–72 hours) and (c) late stages (109–120 hours). Note the persistent translational domain throughout the experiment. (d–f) Map view of incremental horizontal and vertical displacement (Vx, Vz) and strain pattern (ε_{xx}) of Model B from the (d) early (25–36 hours), (e) mid (61–72 hours) and (f) late stages (109–120 hours). Note the delayed deformation and large translational domain in the model. The horizontal displacement (Vx) displays downslope displacement of the sedimentary cover (left to right in map view). The vertical displacement (Vz) displays total subsidence and uplift. ~~Since the monitor system is attached to the apparatus, subsidence indicates net outflow of silicone and uplift indicates net inflow of silicone.~~ The horizontal strain (ε_{xx}) shows location ~~and strain magnitude~~ of the extensional (red) and contractional (purple) structures. ~~The large white space represents the translational domain between the extensional and contractional structures.~~

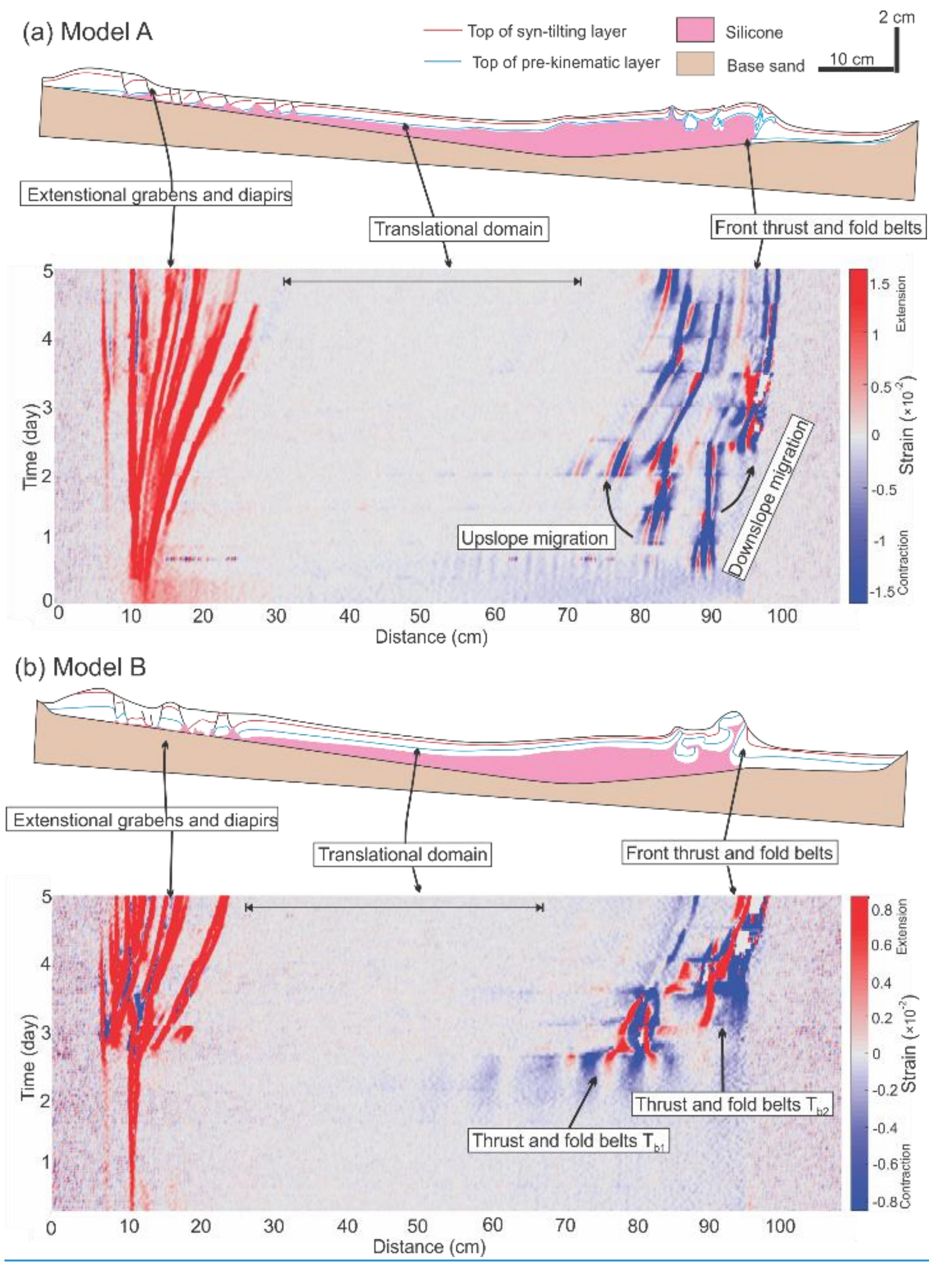

Figure 5. (a) Structural styles and kinematic domain partition in central section of ~~Basin 1a~~Model A. The strain ~~plot of 1hour interval~~evolution diagram (showing incremental strain at 1 hour intervals, or strain rate in 1/h) along the central section beneath shows the initiation of extensional and contractional structures and how they ~~evolved through~~ evolve in space and time. Note the ~~undeformed~~persistent translational domain. (b) Structural styles and kinematic domain partition in central section of ~~Basin 1b~~Model B. The ~~1 hour strain plot through time~~strain evolution diagram (showing incremental strain at 1 hour intervals, or strain rate in 1/h) along the central section shows the evolution of extensional and contractional structures in ~~the central section.~~space and time. Note the ~~contraction~~first contractional structure T_{b1} occur~~red~~s in the mid stage ~~during~~of the experiment.

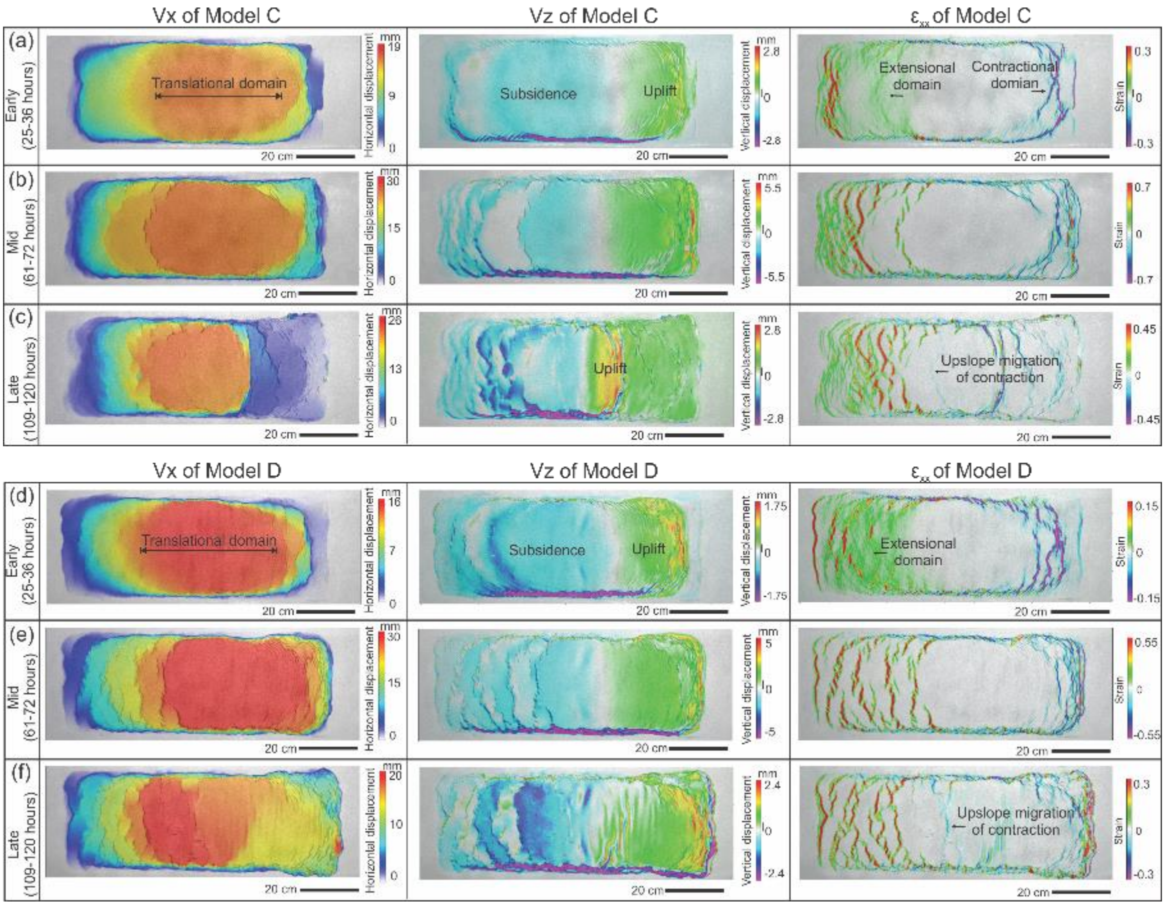

Figure 6. (a–c) Map view of ~~finite~~incremental horizontal and vertical displacement (Vx, Vz) and strain pattern (ε_{xx}) derived from 3D DIC strain data of ~~the experiment 2~~Model C from the (a) early (25–36 hours), (b) mid (61–72 hours) and (c) late stages (109–120 hours). Note the upslope migration of the translational domain and its overprinting at the end of experiment. (d–f) Map view of incremental horizontal and vertical displacement (Vx, Vz) and strain pattern (ε_{xx}) of Model D from the (d) early (25–36 hours), (e) mid (61–72 hours) and (f) late stages (109–120 hours). Note the widely distributed deformation and overprinted translational domain. The horizontal displacement (Vx) displays downslope displacement of the sedimentary cover (left to right in map view). The vertical displacement (Vz) displays total subsidence and uplift. ~~subsidence indicates net outflow of silicone and uplift indicates net inflow of silicone. Note the strings of subsidence of the Basin 2a in the early stage.~~ The horizontal strain (ε_{xx}) shows ~~the~~ location ~~and strain magnitude~~ of the extensional (red) and contractional (purple) structures ~~(purple). Note the basin-wide extension and contraction of the Basin 2b at late stage~~.

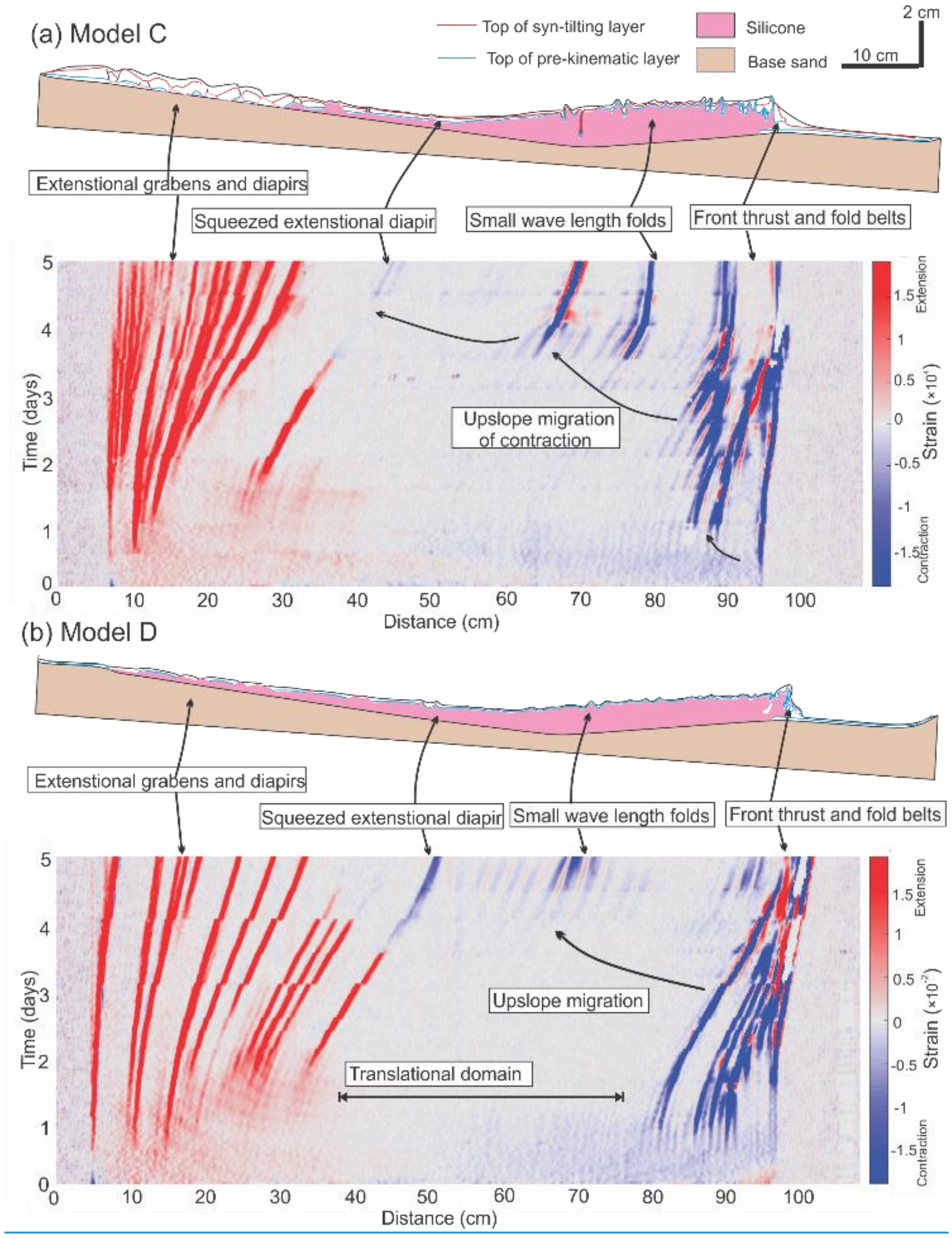

Figure 7. (a) Structural styles and kinematic domain partition in central ~~lo~~se~~ca~~tion of ~~the Basin 2a~~Model C. The strain ~~plot of~~evolution diagram (showing incremental strain at 1 hour ~~interval~~intervals, or strain rate in 1/h) along the central section beneath shows the initiation of extensional and contractional structures and how they ~~evolved through~~ evolve in space and time. Note the ~~basin-wide extension and contraction in the first 6 hours of the experiment when differential loading was intentionally imposed onto the top of the silicone layer. The dash line box indicates the interval enlarged in Fig. 7c.~~squeezed diapir due to the upslope migration of contractional domain. (b) Structural styles and kinematic domain partition in central section of ~~the Basin 2b~~Model D. The strain ~~plot (~~evolution diagram (showing incremental strain at 1 hour ~~interval) through 5 days~~intervals, or strain rate in 1/h) along the central section shows the evolution of extensional and contractional structures ~~along central section. During the later stage the contractional domain migrated upward resulting in small wave length folding in the former~~

~~translational domain. Some extensional diapirs get squeezed in the late stage.~~Note the overall kinematic and structural evolution of Model D are similar to Model A–C despite no differential loading from wedge shaped syn-kinematic sedimentation.

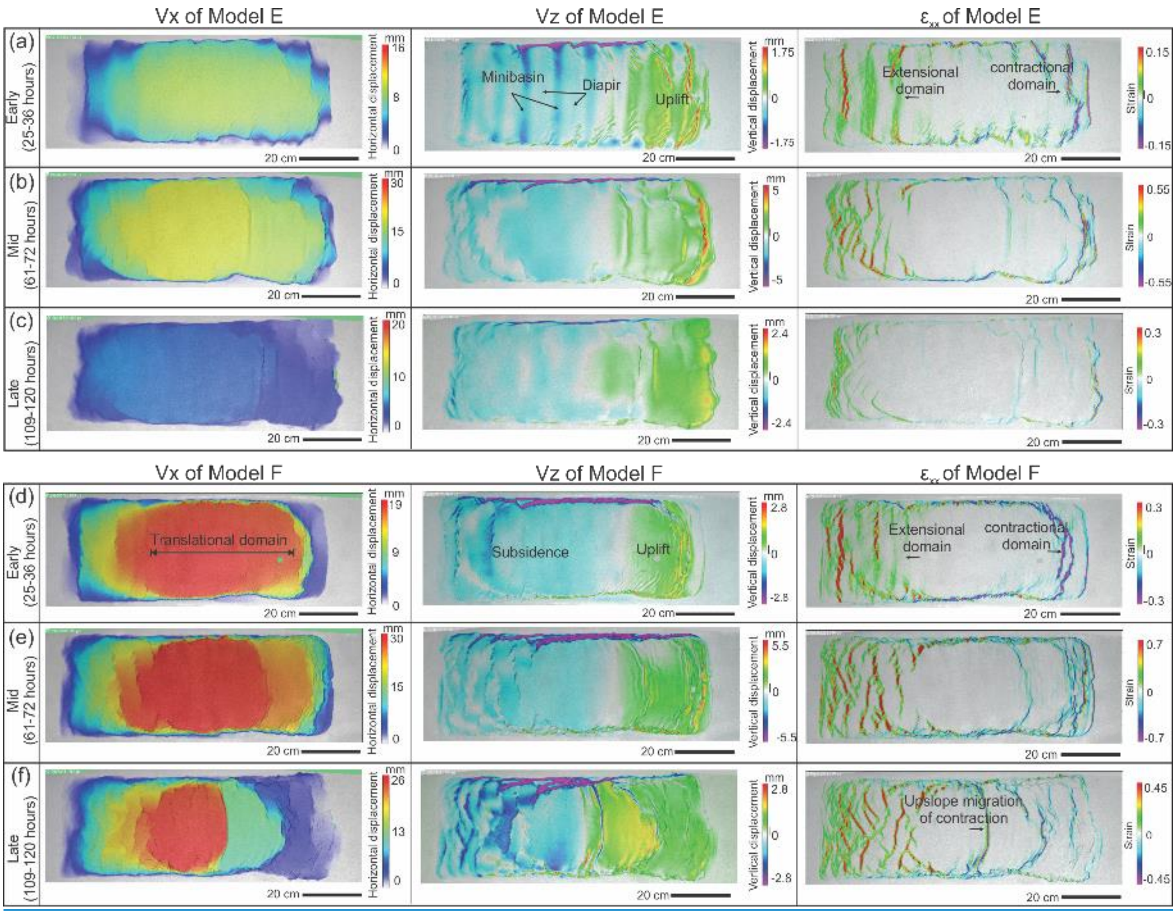

Figure 8. (a–c) Map view of ~~finite~~incremental horizontal and vertical displacement (Vx, Vz) and strain pattern (ε_{xx}) derived from 3D DIC strain data of ~~the experiment 3~~Model E from the (a) early (25–36 hours), (b) mid (61–72 hours) and (c) late stages (109–120 hours). Note the minibasins and diapirs formed in the mid-slope during the early stage of the experiment. (d–f) Map view of incremental horizontal and vertical displacement (Vx, Vz) and strain pattern (ε_{xx}) of Model F from the (d) early (25–36 hours), (e) mid (61–72 hours) and (f) late stages (109–120 hours). Note the overall similarity between Model F to Model C. The horizontal displacement (Vx) displays downslope displacement of the sedimentary cover (left to right in map view). ~~Note the deceasing of the red block from early to late in both basins indicating shrinking of the translational domain.~~ The vertical displacement (Vz) displays total subsidence and uplift. The horizontal strain (ε_{xx}) shows ~~the~~ location ~~and strain magnitude~~ of the extensional (red) and contractional (purple) structures~~. Note the expansion of extension and contraction from early to late in both basins 3a and 3b~~.

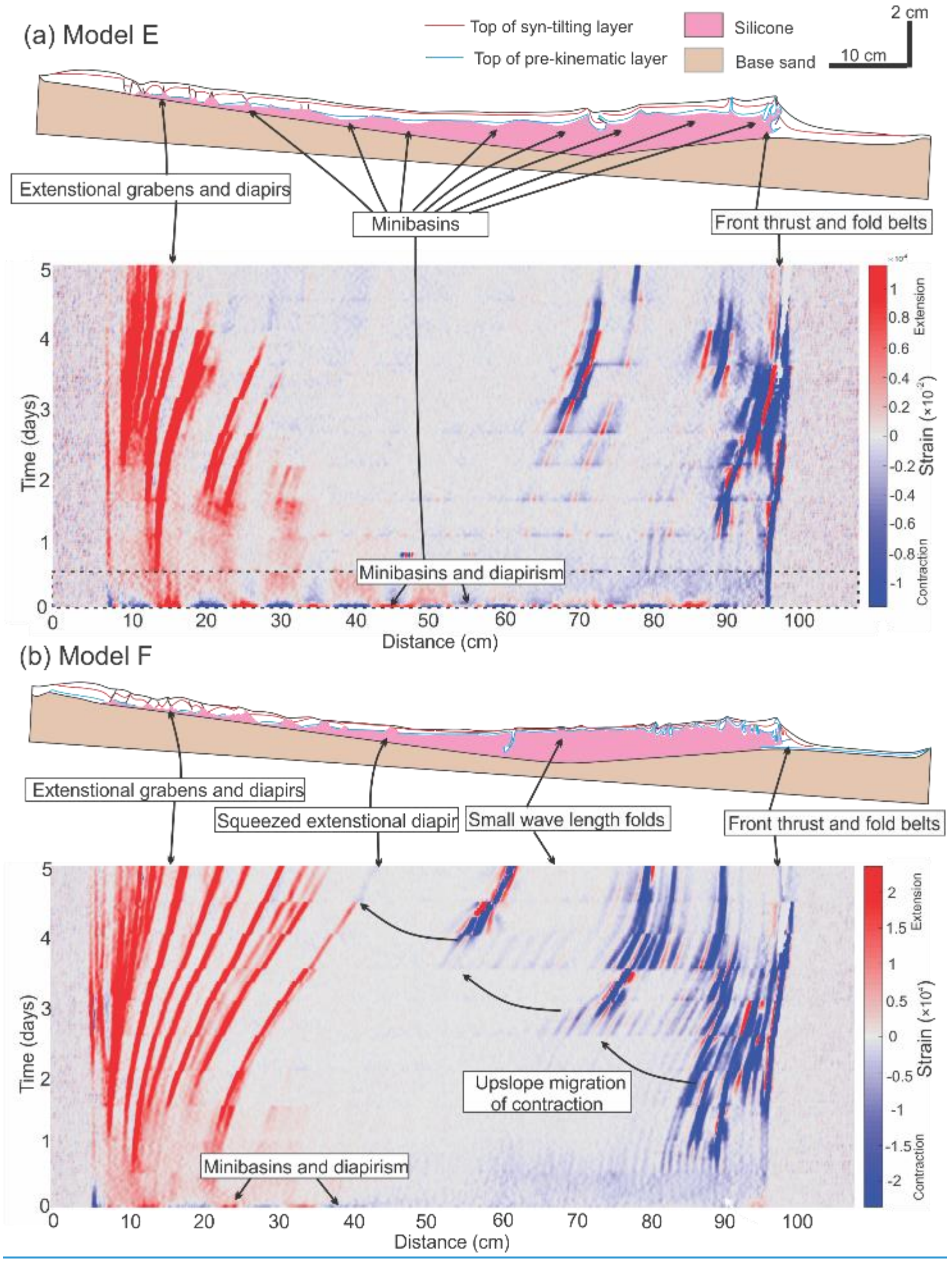

Figure 9 (a) Structural styles and kinematic domain partition in central section of ~~Basin 3a~~Model E. The strain ~~plot of~~evolution diagram (showing incremental strain at 1 hour ~~interval~~intervals, or strain rate in 1/h) along the central section beneath shows the initiation of extensional and contractional structures and how they evolve~~d~~ through time. Note the early stage minibasin formation and diapirism and their imprints in the translational domain area. (b) Structural styles and kinematic domain partition in central section of ~~Basin 3b~~Model F. The strain ~~plot of~~evolution diagram (showing incremental strain at 1 hour ~~interval through 5 days~~intervals, or strain rate in 1/h) along the central section ~~shows~~reveals the evolution of extensional and contractional structures. Note the ~~downslope migration of extensional domain~~early stage diapirism and upslope migration of contraction overprint the translational domain together.

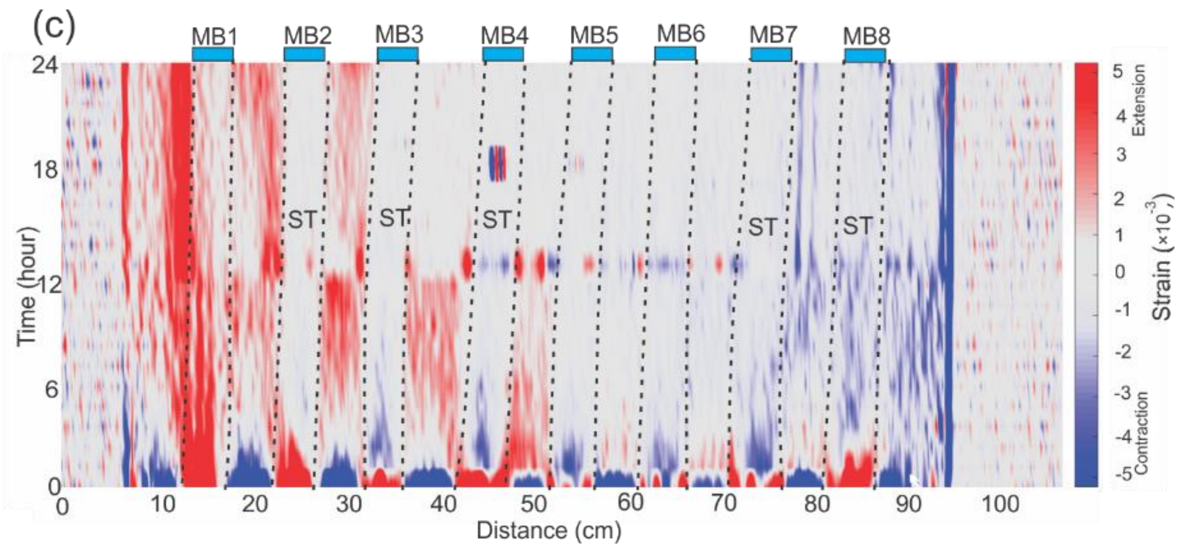

Figure 9 continue. (c) Zoom into the strain evolution diagram for the first 24 hours along centralcross section of Model E. The minibasins gradually change from areas of extension to zones that are relatively strong and stable in the first three hours. MB means minibasin and ST means strain transfer. See Fig. 9a for the strain evolution diagram of the ~~contractional domain in both basins 3a and 3b~~whole experiment of Model E.

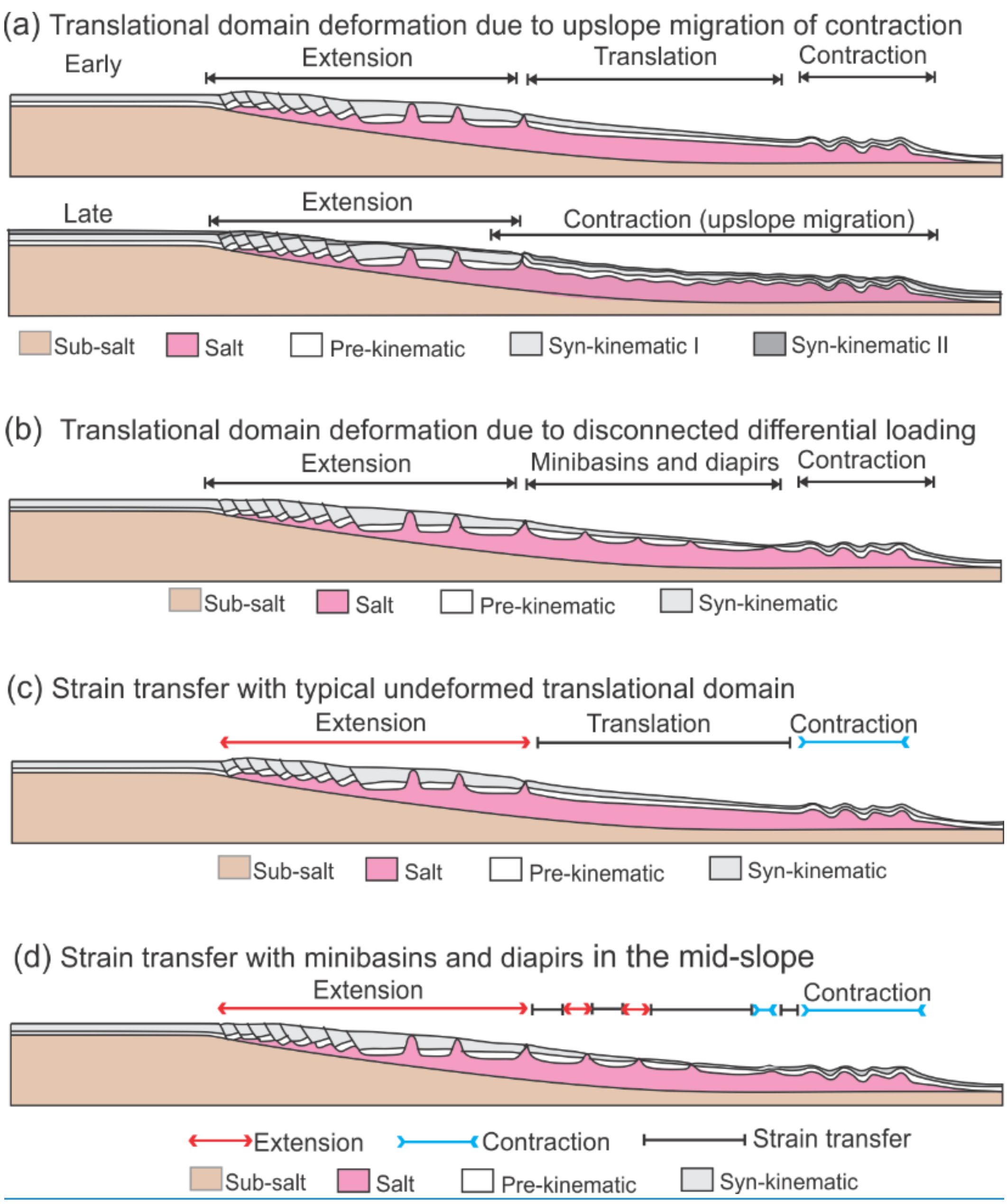

Figure 10. Proposed mechanisms of ~~deforming~~overprinting translational domains and models illustrating strain transfer with underformed translational domain, and ~~minibasin with~~areas of minibasins and diapirs. (a) Low sedimentation rate and thin supra-salt cover allows upslope migration of contraction resulting in ~~deformation of~~overprinting the translational domain. (b) Sedimentary differential loading leads to the development of minibasins and diapirs in the mid-slope preventing the establishment of a stable, undeformed translational domain. (c) The undeformed translational domain in the mid-slope allows strain transfer (ST) without significant internal deformation. (d) The minibasins and diapirs in the mid-slope allow strain transfer (ST) through a combination of passive movement of minibasin and ~~stretching~~minor widening (extension) or ~~squeezing~~shortening (contraction) of diapirs~~ in between~~.

~~Appendix~~

Quantity	Symbol	Unit	Value (model)	Value (prototype)	Scaling relation	Scaling factor
Length	l	m	0.01	1	$l^* = l_{model}/l_{prototype}$	10^{-5}
Density (sediments)	ρ	$kg \cdot m^{-3}$	1130	2400	$\rho^* = \rho_{c\ model}/\rho_{prototype}$	0.47
Gravity acceleration	g	$m \cdot s^{-2}$	9.81	9.81	$g^* = g_{model}/g_{prototype}$	1
Friction coefficient	μ	-	0.55–0.75[#]	0.40–0.80	$\mu^* = \mu_{model}/\mu_{prototype}$	1
Cohesion	C	Pa	35–75[#]	10^{7}	$C^* = C_{model}/C_{prototype} = \rho_c^* l^* g^*$[$]	10^{-5}
Stress	σ	Pa	100	21.30×10^{6}	$\sigma^* = \rho_c^* l^* g^*$	4.70×10^{-6}
Viscosity	η	$Pa \cdot s$	2.00×10^{4} [##]	5.00×10^{18}	$\eta^*=\eta_{model}/\eta_{prototype} = v^{*-1} \rho_v^* l^{*2} g^*$[$$]	4.00×10^{-15}
Strain rate	$d\varepsilon/dt$	s^{-1}	10^{-2}–10^{-7}	10^{-11}–10^{-16}	$(d\varepsilon/dt)^* = \sigma^*/\eta^*$	1.18×10^{9}
Time (submarine)	t	$hour$	1	2.35×10^{9}	$t^* = 1/(2 \cdot d\varepsilon/dt)^*$[§]	4.26×10^{-10}

[#]For static>reactivation>dynamic friction coefficients (Warsitzka et al., 2019)

[##]Rudolf et al. (2016)

[$] brittle regime scaling based on the ratio between lithostatic pressure and cohesion

[$$] viscous regime scaling based on the ratio between lithostatic pressure and viscous strength (Ramberg number), v is a characteristic velocity

[§] submarine systems at hydrostatic conditions deform at about half the rate of subaerial systems (Gemmer et al. 2005) because of the stabilizing effect of the water column and buoyancy. Since the experiment is conducted in sub -aerial environment, we here apply a generic correction factor of 1/2 following Adam et al. (2012a).

Table ~~A1~~1. Material properties and scaling relationship of the experiments in this study. Note geometric scaling of 1cm in model is 1 km in nature and time scaling of 1 hour in model is 0.268 Ma in nature.

Appendix

My	Time in Hr	Sedimentation thickness	Basin 1a	Basin 1b	Basin 2a	Basin 2b	Basin 3a	Basin 3b
			Model A	Model B	Model E	Model D	Model F	Model C
0	0	**Pre-kinematic**	1 mm	5 mm	1 mm with DF	1 mm	0.5 mm with DF	0.5 mm
1	4							
2	8							
3	12	**Syn-sedimentation 1**	1 mm	1 mm	1 mm with DF	0	0.5 mm with DF	0.5 mm
4	16							
5	20							
6	24	**Syn-sedimentation 2**	1 mm	1 mm	1 mm with DF	0	0.5 mm with DF	0.5 mm
7	28							
8	32							
9	36	**Syn-sedimentation 3**	1 mm	1 mm	1 mm with DF	0.14 mm	0.5 mm with DF	0.5 mm
10	40							
11	44							
12	48	**Syn-sedimentation 4**	1 mm	1 mm	1 mm	0.17 mm	0.5 mm	0.5 mm
13	52							
14	56							
15	60	**Syn-sedimentation 5**	1 mm	1 mm	1 mm	0.12 mm	0.5 mm	0.5 mm
16	64							
17	68							
18	72	**Syn-sedimentation 6**	1 mm	1 mm	1 mm	0.2 mm	0.5 mm	0.5 mm
19	76							
20	80							
21	84	**Syn-sedimentation 7**	1 mm	1 mm	1 mm	0.12 mm	0.5 mm	0.5 mm
22	88							
23	92							
24	96	**Syn-sedimentation 8**	1 mm	1 mm	1 mm	0.31 mm	0.5 mm	0.5 mm
25	100							
26	104							
27	108	**Syn-sedimentation 9**	1 mm	1 mm	1 mm	0.27 mm	0.5 mm	0.5 mm
28	112							
29	116							
30	120	Stop	Stop	Stop	Stop	Stop	Stop	Stop

Table ~~A2~~A1. Sedimentation rates, pre- and syn-kinematic depositional scenarios for all six silicone basins of the three experiments~~ m – model, p - prototype~~. Note the labels of basins, such as Basin 1a and 1b, are for paired models. The labels of models are the names referred in the main text.